

Plasmon mechanism of high-temperature superconductivity in cuprate metal-oxide compounds

E. A. Pashitskiĭ

Physics Institute, Ukrainian Academy of Sciences

(Submitted 24 February 1992)

Zh. Eksp. Teor. Fiz. **103**, 867–909 (March 1993)

The plasmon mechanism of Cooper pairing of almost-free “light” carriers in a wide $2D$ band is considered in the framework of standard superconductivity theory in the intermediate-coupling approximation. The model used is that of a layered metal with quasi-two-dimensional electron spectrum and a narrow band near the Fermi level, with exchange of virtual quanta of low-frequency collective excitations of the charge density of almost localized “heavy” carriers in a narrow $2d$ -band (acoustic plasmons), which are hybridized with dipole-active oxygen vibrational mode (optical phonons) in the entire volume of the Brillouin band. It is shown that when account is taken of the multilayer structure of cuprate metal-oxide compounds and of multiparticle Coulomb correlations (of the type of “local-field” effects), such a mechanism can ensure quite high values of the critical temperature of the superconducting transition temperature T_c and describes correctly all the main properties of high-temperature superconductors, such as the nonmonotonic dependence of T_c on the density of the doping impurity or on the oxygen content, the rise of T_c with increase of the number n of the cuprate CuO_2 layers in the primitive cell of the crystal with a tendency to saturation at $n \geq 3$, the anomaly of the oxygen isotopic effect, and others.

1. INTRODUCTION

1. It is known¹ that high-temperature superconductors based on cuprate metal-oxide compounds (MOC) have many unusual physical properties, including: a) anomalously high critical superconducting (SC) transition temperatures^{2–6} $T_c \approx (30–125)$ K at optimal composition, b) an anomalously weak isotopic effect (IE) which tends to decrease with increase of T_c (Refs. 7–10), c) a nonmonotonic dependence of T_c on the density of the dopant and on the oxygen content, i.e., on the density of the carriers (holes, electrons) in the conducting CuO_2 layers,^{11–15} d) rise of T_c with increase of the number n of the cuprate layers in the primitive cell of the crystals,^{16–18} e) correlation between the maximum values of T_c and the frequencies of the “oxygen” vibrational modes for various classes of cuprate MOC,^{19,20} and others.

It will be shown below that all the above as well as other features of high-temperature superconductivity (HTSC) in cuprate MOC can be explained (at least qualitatively) on the basis of a simple model, proposed in Refs. 21 and 22, of a layered metal with overlapping and partially filled wide and narrow two-dimensional ($2D$) bands near the Fermi level.¹¹

2. In an anisotropic spectrum of collective electron excitations of a two-band quasi-two-dimensional metal with light (l) and (h) carriers (electrons, holes) there exists a low-frequency (l f) oscillation mode of the h -carrier charge density, with a quasi-acoustic dispersion law, called acoustic plasmons (AP), the possible existence of which had been discussed earlier^{23–26} as applied to transition metals and their compounds, semimetals, and semiconductors.

In contrast to metals (or semiconductors), however, which have relatively wide bands (valleys) and a quadratic spectrum of degenerate l - or h -carriers, when the AP mode is bounded on the high-momentum side by a region of strong Landau quantum damping,^{23,24} in layered metals with very narrow $2D$ bands, for which the spectrum takes the form

$$E_h(k_x, k_y) = \frac{W_h}{4} (\cos k_x a + \cos k_y b), \quad (1)$$

where W_h is the band width, and a and b are the lattice constants in the plane of the layers ($a \approx b \ll c$), the AP branch lies higher than the upper boundary of the region of strong Landau damping by h -carriers in the entire volume of the Brillouin zone (BZ)²¹ under certain conditions (particularly when

$$W_h < e^2/a\epsilon_\infty,$$

where ϵ_∞ is the high-frequency (hf) dielectric constant of the crystal.

In other words, in the strong coupling approximation, which corresponds to h -carriers almost localized on the sites of the crystal lattice and consequently to a periodically inhomogeneous distribution of the electron density, the h -plasmon spectrum $\omega_h(\mathbf{q})$ is a periodic function of the quasimomentum having the period of the reciprocal lattice (similar to the phonon spectrum). Therefore the real part of the effective permittivity $\tilde{\epsilon}(\mathbf{q}, \omega)$ of the metal is negative in the energy region

$$W_h \sin(q_{\parallel} a/2) < |\omega| < \omega_h(\mathbf{q})$$

in the entire range $q_{\parallel} \leq 2k_{F1}$ of importance for l -carrier Cooper pairing (k_{F1} is the Fermi momentum of the degenerate l -carriers). That is to say, attraction appears in the screened Coulomb interaction (SCI) and is due to exchange of virtual AP:

$$\text{Re } \tilde{V}_C(\mathbf{q}, \omega) \equiv V_C(\mathbf{q}) \text{Re } \tilde{\epsilon}^{-1}(\mathbf{q}, \omega) < 0, \quad (2)$$

where V_C is a matrix element of unscreened Coulomb repulsion.

This attraction, due to the “dynamic rescreening” effect on account of the retarded electron-plasmon interaction

(EPI), contributes to the superconductivity and is characterized, in view of the Kramers–Kronig relation for the response function^{28,29} $\tilde{\epsilon}^{-1}(\mathbf{q}, \omega)$ by the dimensionless coupling constant

$$\lambda_{pl} = -\frac{2}{\pi} \nu_l \int_0^{\infty} \frac{d\omega}{\omega} \langle V_C(\mathbf{q}) \text{Im} \tilde{\epsilon}^{-1}(\mathbf{q}, \omega) \rangle, \quad (3)$$

where ν_l is the density of states (DS) on the Fermi level in a wide 2D band (of width $W_l \gg W_h$), and the angle brackets $\langle \dots \rangle$ denote averaging over a weakly rippled cylindrical Fermi surface (FS). The increase of λ_{pl} compared with the constant λ_{ph} of the electron-phonon interaction (EPI) leads on the one hand to an increase of T_c and on the other to a suppression of the IE (see Ref. 21), in qualitative agreement with the experimental data.^{9,10}

3. It must be emphasized that the feasibility of a “plasmon” mechanism of superconductivity was considered theoretically long before the discovery³⁰ of HTSC for transition metals and their alloys and compounds,^{26,31,33} and also for degenerate multivalley semiconductors, semimetals, and layered semiconductor structures (Refs. 34–36).³⁾

This mechanism is being discussed of late as one of the possible causes of HTSC in cuprate MOC (see, e.g., Refs. 38–43). It must be borne in mind here, however, that in single-band layered metal, notwithstanding the quasicoustic dispersion law for long-wave plasma oscillations propagating across the layers (see Refs. 39 and 41), the energies of virtual plasmons in the region of large momentum transfers (of the order of the Fermi momentum k_F) exceed the Fermi energy E_F , so that their contribution to the attraction near the FS, and hence in the Cooper-pairing mechanism, is suppressed by quasiparticle damping.²⁸

As shown in Refs. 34 and 44 (see also Refs. 21 and 42), in multiband metals or in multivalley degenerate semiconductors (semimetals) with l and h carriers the ECI effectiveness can increase substantially in the case of strong ion coupling, when the static permittivity of the crystal is $\epsilon_0 \gg \epsilon_{\infty}$. In this case, owing to hybridization of the AP with the optical longitudinal (LO) and transverse (TO) phonons, the interelectron attraction region broadens in energy all the way to

$$\omega \approx \sqrt{\omega_{LO}^2 + \Omega_h^2},$$

where ω_{LO} is the LO-phonon frequency and Ω_h is the plasma frequency of the h -carriers. In this case, however, the attraction-region upper-bound momentum remains the same

$$q_{max} \approx \sqrt{\omega_{LO}^2 + \Omega_h^2} / v_{Fh}$$

(see Fig. 1a) if the spectrum of the degenerate h -carriers with Fermi velocity v_{Fh} is quadratic. The attraction region can broaden substantially if the h -carriers form a Wigner crystal and the spectrum of their collective excitations (phonons) becomes a periodic function of the quasimomentum.⁴⁾

4. In a layered metal with a narrow 2D band in an essentially nonparabolic h -carrier spectrum the AP spectrum remains by definition periodic in q_{\parallel} (with a period $2\pi/a$), and the hybridization of the AP with the LO and TO phonons proceeds over the entire BZ volume (Fig. 1b), so that an attraction between the l -carriers in region (1) exists over the entire momentum-transfer interval $0 \leq q \leq 2k_{F1}$, where k_{F1}

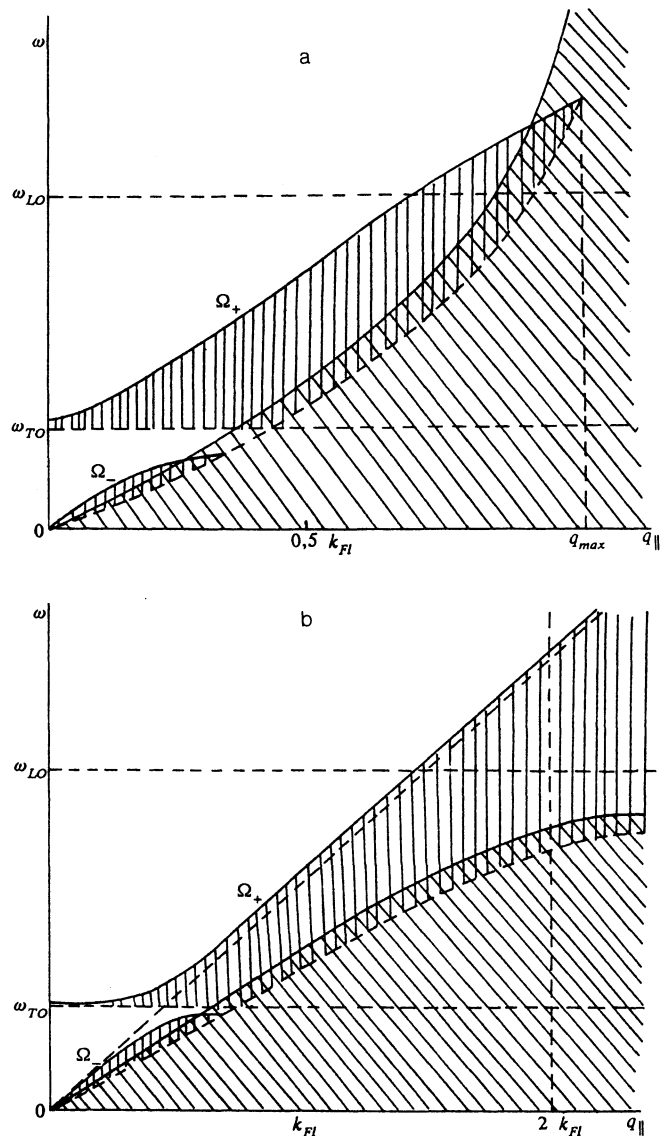


FIG. 1. Spectrum of hybrid phonon-plasma oscillations (solid curves) in a layered ionic crystal with $\omega_{TO}/\omega_{LO} = 0.3$ ($\epsilon_{\infty}/\epsilon_0 = 0.09$) with a quadratic h -carrier spectrum (a) and with a nonparabolic (cosinusoidal) spectrum in a narrow 2D band (b) for oblique propagation of oscillations with a transverse wave number $q_z = \pi/2d$ (for $\alpha_{\infty} = 2$ and $k_{F1} d = 4$). Oblique hatches show the regions of strong quantum Landau damping by h -carriers in which $\text{Im} \epsilon(q, \omega) > 0$. Vertical hatches show regions of effective (retarding) attraction, in which $\text{Re} \tilde{\epsilon}(q, \omega) < 0$.

$= \sqrt{2\pi N_l}$ is the Fermi momentum of the l -carriers and N_l is their surface 2D density in the layer. We assume hereafter that in cuprate MOC the most effectively hybridized with the AP are those optical phonon modes corresponding to oscillations of the oxygen ions O^{2-} in the CuO_2 layers. This explains, in particular, the experimentally observed the shift, and the broadening into the hf region, of the corresponding peaks of the “phonon” DS determined from tunnel experiments⁴⁶ or from inelastic neutron scattering^{47,48} in transitions from non-superconducting or low-temperature superconducting phase of cuprate MOC to HTSC phases.

The assumption of a predominant role of such a hybrid phonon-plasma mode in the mechanism of Cooper pairing of l -carriers explains also the linear connection, revealed^{19,20} by MOC Raman optical spectra, between the maximum values of T_c and the frequencies $\tilde{\Omega}_+ \approx 2\pi T_c^{\max}$, of the corre-

sponding vibrational modes, which is typical of the single-mode spectrum.⁴⁹

The monotonic increase of the h -carrier density in the course of doping of cuprate MOC by a non-isovalent impurity or by changing the composition and the oxygen content⁵¹ leads, in the framework of the described model, to a non-monotonic change of T_c , since the increase of the plasma frequency Ω_h and the broadening of the attraction region take place simultaneously with an enhancement of the Coulomb repulsion on account of the decrease of the Bogolyubov–Tolmachev logarithm⁵² in the Morel–Anderson pseudopotential.⁵³ Such a T_c dependence with a maximum at a certain optimal carrier density agrees qualitatively^{11–15} with experiment.⁶⁾

Finally, by taking into account the specific features of the Coulomb interaction and of the “local-field” effects, in multilayer structures with a spatially inhomogeneous electron-density distribution in a direction perpendicular to the plane of the layers (along the $c||z$ axis) we can obtain, within the framework of the proposed ECI model, high $T_c \gtrsim 100$ K and the dependence of T_c on the number n of the cuprate CuO_2 layers in the unit cell of the crystal, in good agreement with the experimental data for MOC of the type, $\text{Bi}_2\text{Sr}_2\text{Ca}_{n-1}\text{Cu}_n\text{O}_x$, and $\text{Tl}_m\text{Ba}_2\text{Ca}_{n-1}\text{Cu}_n\text{O}_x$ ($m = 1, 2$) (Refs. 16–18), and also for $(\text{Ca}_{1-x}\text{Sr}_x)_{1-y}\text{CuO}_2$ (Ref. 54).

2. ELECTRON-PLASMON-INTERACTION AND ELECTRON-PHONON-INTERACTION MODEL IN LAYERED METAL-OXIDE COMPOUNDS

1. We examine the “plasmon” mechanism of HTSC in cuprate MOC by starting with a simple model of the band spectrum of a layered metal with two partially filled overlapping $2D$ -bands of substantially different width ($W_l \gg W_h$) near the Fermi level. Such a model was used²² to describe qualitatively correctly the various anomalous properties of the metallic phases of cuprate MOC in the normal state, in particular: a) the almost linear temperature dependences of the electric resistivity⁵⁵ and of the reciprocal Hall constant⁵⁶ with allowance for the inelastic scattering of the majority degenerate l -carriers in a wide $2D$ band damping acoustic plasmons and the finite contribution made to the conductivity by nondegenerate h -carriers in a narrow $2D$ band; b) the presence of a dip (minimum) in the frequency dependence of the optical conductivity of MOC in the infrared (IR) band⁵⁷ as an analog of the Holstein effect on phonons due to renormalization of the quasiparticle spectrum as a result of the electron-plasma interaction; c) the deviation from the Korringa law for the relaxation rate of the nuclear spins of copper ions⁵⁸ due to their interaction with collective excitations of the spin density of h -carriers (paramagnons), and others.

The assumed presence, in the electron spectrum of cuprate MOC, of a narrow band with a high state density is indirectly confirmed by the “pinning” of the Fermi level in the photoelectron emission and x-ray absorption spectra^{50,51,59} in the course of doping. Detailed numerical calculations^{60–64} of the band structure of cuprate MOC, with allowance for hybridization of a large number of atomic orbitals and for correlation (exchange) effects, likewise point to the possible appearance of sufficiently narrow $2D$ bands near the FS. Furthermore, these bands can become consider-

ably narrowed by correlation effects or by polaron narrowing, i.e., an increase of the h -carrier mass by their interaction with 1f phonons (see Ref. 65).

2. The presence of a narrow $2D$ band (of width $W_h \lesssim 0.05$ eV) against the background of a much broader W_l (of width $W_l \gtrsim 1$ eV) produces, as noted above, in the spectrum of the collective excitations of the l - and h -carriers, a weakly damped AP mode, which becomes hybridized with the optical phonon modes in the entire BZ volume (Fig. 1b). We assume hereafter that hybridization in cuprate MOC is most effective for those phonon modes which correspond to vibrations of the oxygen O^{2-} ions in the CuO_2 layers where the l - and h -carriers are localized. According to tunnel⁴⁶ and neutron^{47,48} experiments the frequencies of such hybrid vibrations shift to the higher-frequency region on going from the non-superconducting or low-temperature superconducting phases of the cuprate MOC (such as $\text{YBa}_2\text{Cu}_3\text{O}_6$ and $\text{Bi}_2\text{Sr}_2\text{CuO}_6$) into high-temperature SC phases.

In this case the retarded interaction between the l -carriers, due to exchange of virtual quanta of hybrid phonon-plasma vibrations, jointly with screened Coulomb repulsion in the momentum-transfer region $q_{||} \lesssim 2k_{\text{F}l}$ and $q_z \lesssim \pi/d$ and under the condition $K_{\text{F}l}a \lesssim 1$ can be described in the framework of the so-called generalized “jellium” model^{29,66}:

$$\tilde{V}_{ll}(\mathbf{q}, \omega) = \frac{V_C(\mathbf{q})}{\varepsilon(\mathbf{q}, \omega)} \equiv D_{pl}(\mathbf{q}, \omega) + \text{Re} \frac{V_C(\mathbf{q})}{\varepsilon(\mathbf{q}, \omega_{\text{max}})}, \quad (4)$$

where

$$D_{pl}(\mathbf{q}, \omega) = V_C(\mathbf{q})[\tilde{\varepsilon}^{-1}(\mathbf{q}, \omega) - \text{Re} \tilde{\varepsilon}^{-1}(\mathbf{q}, \omega_{\text{max}})]$$

is the plasmon Green’s function^{21,22} ω_{max} is the maximum interaction cutoff energy (more below), and $\tilde{\varepsilon}(\mathbf{q}, \omega)$ is the effective permittivity of the metal given, with allowance with the spatial and temporal dispersion but without allowance for interband hybridization, by

$$\tilde{\varepsilon}(\mathbf{q}, \omega) = \varepsilon_i(\mathbf{q}, \omega) - V_C(\mathbf{q})[\tilde{\Pi}_l(\mathbf{q}, \omega) + \tilde{\Pi}_h(\mathbf{q}, \omega)] - \frac{\omega_0^2(\mathbf{q})g_0^2(\mathbf{q})/V_C(\mathbf{q})}{\omega^2 - \omega_0^2(\mathbf{q})[1 - g_0^2(\mathbf{q})/V_C(\mathbf{q})]}. \quad (5)$$

Here ε_i is the permittivity component connected with the polarization of the ion lattice and with the interband transitions (see Ref. 67), $\tilde{\Pi}_l$ and $\tilde{\Pi}_h$ are the polarization operators of the l - and h -carriers with allowance for structural and correlation effects (more below), g_0 is the EPI matrix element for the “oxygen” phonon mode with bare frequency ω_0 , and V_C is the Coulomb matrix element. In a layered crystal with n packets of conducting layers in each unit cell (Fig. 2) with distance d_0 between cells and distance d between packets,⁷⁾ under the conditions $q_{||}d \gg 1$ and $q_{||}d_0 \gg 1$ but $q_{||}a \ll \pi$, this matrix element takes the form (see the Appendix)

$$V_C(q_{||}, n) \approx \frac{2\pi e^2}{q_{||}} c(n), \quad c(n) = d + (n - 1)d_0. \quad (6)$$

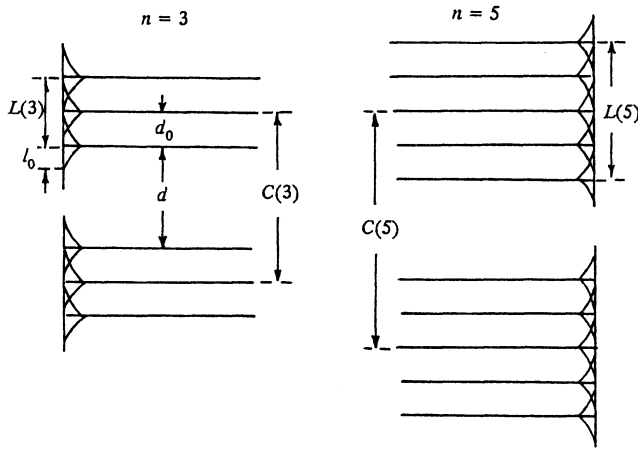


FIG. 2. Arrangement of CuO_2 layers of multilayer cuprate MOC of type $\text{TlBa}_2\text{Ca}_{n-1}\text{Cu}_n\text{O}_x$ with $d = 9.6 \text{ \AA}$ and $d_0 = 3.2 \text{ \AA}$ for $n = 3$ and 5 . The curves show schematically the distribution of the electron density, which decreases exponentially with increasing distance from the plane of a layer with characteristic length $l_0 \ll d$.

3. If the probability of electron tunneling between neighboring layers is low enough, so that the variables of the "fast" longitudinal motion of the l - and h -carriers in the layer plane and of the "slow" adiabatic transverse motion separate,⁸⁾ the corresponding PO take the form

$$\tilde{\Pi}_{l,h}(\mathbf{q}, \omega, n) \approx \Pi_{l,h}(\mathbf{q}, \omega) \tilde{\beta}(n) d / c(n), \quad (7)$$

where $\tilde{\beta}(n)$ is a structure factor that take into account the spatially inhomogeneous distribution of the electron density along the $c \parallel z$ axis (see the Appendix and Fig. 3).

In the energy ω and momentum q_{\parallel} transfer region defined by the conditions

$$W_h \sin(q_{\parallel} d / 2) < |\omega| < \min\{q_{\parallel} v_{F1}, \Omega_l\}, \quad c^{-1}(n) < q_{\parallel} < \pi / a, \quad (8)$$

where v_{F1} is the Fermi velocity of the l -carriers, and Ω_l is their plasma frequency, we have in the random-phase approximation (RPA)

$$\text{Re } \Pi_l \approx -2\nu_l / d, \quad \text{Re } \Pi_h \approx \frac{q_{\parallel}^2}{4\pi e^2} \frac{\Omega_h^2}{\omega^2}. \quad (9)$$

Here $\nu_l = m_l^* / 2\pi$ is the density of states of the degenerate l -carriers near the edge of the relatively wide $2D$ band, $m_l^* = 4/a^2 W_l$ is their effective mass, and Ω_h is the plasma frequency of the h -carriers (see Ref. 22).

The real part of the permittivity $\tilde{\epsilon}$ (5) can then be approximately represented, in the frequency region $W_h \lesssim |\omega| \ll \Omega_l$, where there is no strong Landau damping by the h -carriers, and the Landau damping by the l -carriers is small, in the form

$$\text{Re } \tilde{\epsilon}(\mathbf{q}, \omega) \approx \left[1 + \frac{2\tilde{\beta}(n)}{q_{\parallel} a_l^*} \right] \frac{[\omega^2 - \Omega_+^2(\mathbf{q})][\omega^2 - \Omega_-^2(\mathbf{q})]}{\omega^2 [\omega^2 - \omega_{TO}^2(\mathbf{q})]}, \quad (10)$$

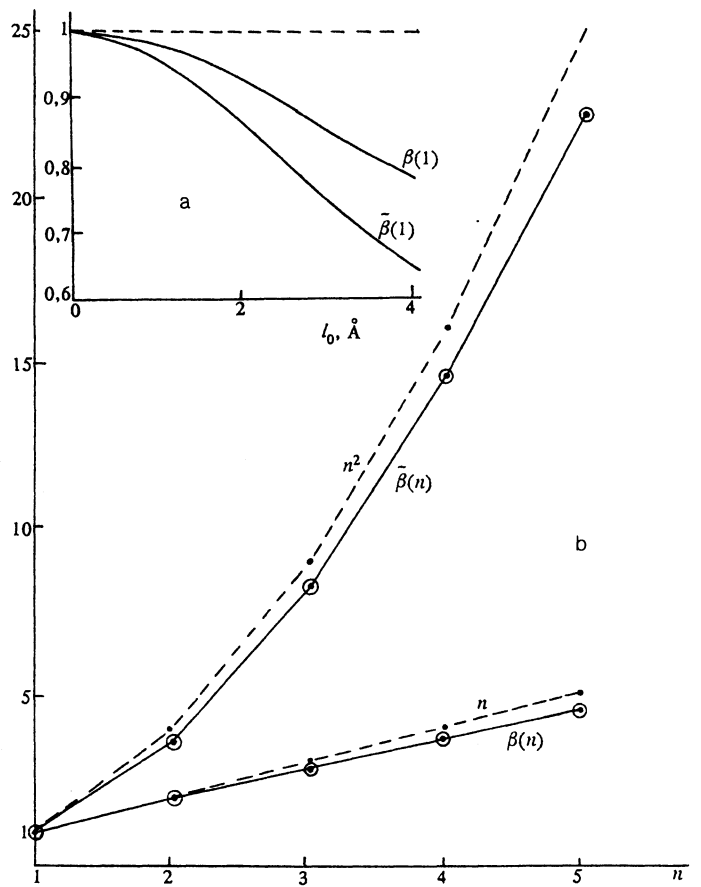


FIG. 3. Dependences of the structure factors $\beta(1)$ and $\tilde{\beta}(1)$ on l_0 at $d = 12 \text{ \AA}$ (a) and dependences of $\beta(n)$ and $\tilde{\beta}(n)$ on n at $d = 12 \text{ \AA}$ and $d_0 = 3.2 \text{ \AA}$ at the limit $l_0 = 0$ (b).

where

$$\Omega_{\pm}(\mathbf{q}) = \left\{ \frac{1}{2} [\omega_h^2(\mathbf{q}) + \tilde{\omega}_{LO}^2(\mathbf{q}) + \omega_{TO}^2(\mathbf{q})] \pm \sqrt{\frac{1}{4} [\omega_h^2(\mathbf{q}) + \tilde{\omega}_{LO}^2(\mathbf{q}) + \omega_{TO}^2(\mathbf{q})]^2 - \omega_h^2(\mathbf{q}) \omega_{TO}^2(\mathbf{q})} \right\}^{1/2}, \quad (11)$$

$$\omega_h(\mathbf{q}) = \Omega_h \left\{ \tilde{\beta}(n) \frac{q_{\parallel} d}{2} \left[1 + \frac{2\tilde{\beta}(n)}{q_{\parallel} a_l^*} \right]^{-1} \right\}^{1/2}, \quad (12)$$

$$\tilde{\omega}_{LO}(\mathbf{q}) = \left[\frac{\omega_{LO}^2(\mathbf{q}) - \omega_{TO}^2(\mathbf{q})}{1 + 2\tilde{\beta}(n) / q_{\parallel} a_l^*} \right]^{1/2}, \quad (13)$$

$$\omega_{LO}(\mathbf{q}) \equiv \omega_0(\mathbf{q}), \quad \omega_{TO}(\mathbf{q}) = \omega_0(\mathbf{q}) \left[1 - \frac{g_0^2(\mathbf{q})}{V_C(\mathbf{q})} \right]^{1/2}. \quad (14)$$

Here $a_l^* = \epsilon_{\infty} / m_l^* e^2$ is the effective Bohr radius of the l -carriers, and $\epsilon_i \approx \epsilon_{\infty}$ at frequencies higher than those of the polar optical phonons (but low compared with the frequencies of the interband transitions).

As follows from (10), in the regions of ω and q_{\parallel} defined by the inequalities

$$\left\{ \begin{array}{l} \max(\omega_{TO}(q), W_h \sin(q_{\parallel} a/2)) < |\omega| < \Omega_+(q), \\ W_h \sin(q_{\parallel} a/2) < |\omega| < \Omega_-(q), \end{array} \right. \quad (15)$$

we have $\text{Re } \tilde{\varepsilon}(q, \omega) < 0$, i.e., a retarded interelectron attraction takes place:

$$\text{Re } V_{ll}(q, \omega) \equiv V_C(q) \text{Re } \tilde{\varepsilon}^{-1}(q, \omega) < 0.$$

The main contribution to the Cooper pairing of the l -carriers is made by the attraction region due to the exchange of virtual quanta of hybrid phonon-plasma oscillations of frequency

$$\Omega_+(q) \approx [\omega_h^2(q) + \tilde{\omega}_{LO}^2(q)]^{1/2}$$

at $\omega_{LO}^2 \gg \omega_{TO}^2$ [see Eq. (11)].

The retarded EPHI with the remaining phonon modes having frequencies $\omega_j(q)$ and matrix elements $g_j(q)$ can be described with the aid of the usual Green's function:^{29,66}

$$D_{ph}(q, \omega) = \sum_j \frac{g_j^2(q) \omega_j^2(q)}{\omega^2 - \omega_j^2(q)}. \quad (16)$$

3. EQUATION FOR THE GAP PARAMETER AND THE EPI CONSTANT

1. The present opinion is¹ that a change of the oxygen content in a layered cuprate MOC leads to a Hubbard or Mott insulator-metal phase transition that coincides practically with the transition that takes into the HTSC phase when the hole density in the volume of the unit cell is $0.05 < x_p < 0.5$ per CuO_2 layer.¹⁴

We assume henceforth that at the point of transition into the metallic phase ($x_p \approx 0.05$) the Fermi level is in the immediate vicinity of the edge of a narrow 2D band located at a distance E_0 from the nearest edge of a broad 2D band (see Refs. 21 and 22), i.e., the Fermi energy of degenerate l carriers is $E_{Fl} \approx E_0 < W_l/2$ but $E_0 \gg W_h$). In the doping process, for like type of l and h carriers (electrons or holes), as the narrow band is filled at high density of states ($\nu_h \gg \nu_l$) the position of the Fermi level and the density of the l -carriers remain practically unchanged, whereas the density N_h of the h -carriers and their plasma frequency Ω_h increase.

It is assumed also that to describe practically free degenerate l -carriers one can use the standard Fermi-liquid approach (with allowance for the quasi-two-dimensional character of the electron spectrum) and for the usual Cooper pairing mechanism in the superconducting state at $T \lesssim T_c$. At the same time, almost-localized h -carriers can remain nondegenerate all the way to $T \ll T_c$ (see Refs. 21 and 22).

2. In this two-component model, the integral equation for the SC order parameter of l -carriers, linearized for $T \rightarrow T_c$ and with allowance for the "local-field" and "anomalous" vertex-parts effects⁶⁸ takes the form

$$\begin{aligned} \Delta_l(p, i\omega_n) &= T_c \sum_{\omega_m} \int \frac{d^3 p'}{(2\pi)^3} \mathcal{G}_l(p', i\omega_m) \\ &\times [D_{ph}(p' - p, i\omega_m - i\omega_n) + \tilde{V}_{ll}(p' - p, i\omega_m - i\omega_n)] \\ &\times \Gamma_C^2(p', i\omega_m; p, i\omega_n; p' - p, i\omega_m - i\omega_n). \end{aligned} \quad (17)$$

Here $\omega_n = (2n + 1)\pi T_c$ are discrete "frequencies" ($n = 0, \pm 1, \pm 2, \dots$), Γ_C is the normal Coulomb (three-pole) vertex,⁹⁾ and \mathcal{G}_l is the Gor'kov anomalous temperature function,⁷⁰ which takes in the case of a weak ripple of the cylindrical Fermi surface in a layered medium and in the case of separable (in the adiabatic approximation) variables of the longitudinal and transverse motion of the l -carriers in 2D-layers, the form

$$\begin{aligned} &\mathcal{G}_l(p_{\parallel}, p_{\perp}, i\omega_n) \\ &= \frac{\Delta_l(p_{\parallel}, i\omega_n) \Psi_{\perp}^2(p_{\perp})}{[i\omega_n - \tilde{\xi}_l(p_{\parallel}) - f_l(i\omega_n)] [i\omega_n + \tilde{\xi}_l(p_{\parallel}) - f_l(i\omega_n)]}, \end{aligned} \quad (18)$$

where $\Psi_{\perp}^2(p_{\perp})$ is the Fourier component of the squared transverse part $\Psi_{\perp}(z)$ of the l -carrier wave function in the layer (see the Appendix), $\tilde{\xi}_l(p_{\parallel})$ is the energy of the longitudinal motion in the plane of the layer, reckoned from the Fermi level renormalized by the interelectron interaction

$$\tilde{E}_{Fl} = E_{Fl} - \Sigma_l(k_{Fl}, 0),$$

and Σ_l is the self-energy part, defined by the integral equation

$$\begin{aligned} \Sigma_l(p, i\omega_n) &= T_c \sum_{\omega_m} \int \frac{d^3 p'}{(2\pi)^3} G_l(p', i\omega_m) \\ &\times [D_{ph}(p' - p, i\omega_m - i\omega_n) + \tilde{V}_{ll}(p' - p, i\omega_m - i\omega_n)] \\ &\times \Gamma_C(p', i\omega_m; p, i\omega_n; p' - p, i\omega_m - i\omega_n). \end{aligned} \quad (19)$$

Here G_l is the normal Green's function of the l -carriers:

$$G_l(p_{\parallel}, p_{\perp}, i\omega_n) = \frac{\Psi_{\perp}^2(p_{\perp})}{i\omega_n - \tilde{\xi}_l(p_{\parallel}) - f_l(i\omega_n)}. \quad (20)$$

and $f_l(i\omega_n)$ is the part of $\Sigma_l = \Sigma_{ph} + \Sigma_C$ which is odd with respect to the sign of ω_n .

The Coulomb vertex Γ_C is known to satisfy on the FS of a charged Fermi liquid the Ward-Pitaevskii identity (see Ref. 70) which takes, in the presence of LF collective (plasma) excitations of the charge density the form (see Ref. 21)

$$\Gamma_C^0 \equiv 1 - \frac{\partial \Sigma_C(\omega)}{\partial \omega} \Big|_{\omega=0} = 1 - \frac{\partial f_{pl}(\omega)}{\partial \omega} \Big|_{\omega=0}, \quad (21)$$

where $f_{pl}(\omega)$ is that part of the function $f_l(\omega)$ which is due to the EPI (see below).

Changing in (17) from integration over p'_\parallel to an integral over

$$\xi' \equiv \tilde{\xi}(p'_\parallel)$$

from $-\infty$ to $+\infty$ accurate to terms of order $(T_c/\tilde{E}_{F1})^2$ and recognizing that the residue at the pole with respect to ξ' in the anomalous Green's function (18) has a singularity ($\sim 1/\omega_m$) at small $\omega_m = \pi T_c$, we see that near the FS ($\omega_n = \pi T_c$, $p_\parallel \approx p'_\parallel \approx k_{F1}$), under the condition that Γ_C depends little on the energy transfers $|\omega_m - \omega_n|$ and momentum transfers $q = |\mathbf{p}' - \mathbf{p}|$, the square of the vertex part Γ_C^2 contained in (17) can be approximately replaced by $(\Gamma_C^0)^2$. We shall henceforth use Γ_C^0 to replace only one ("excess") vertex Γ_C in (17), and neglect for simplicity the contribution of the remaining vertices Γ_C in (17) and (19), since the vertex Γ_C tends to unity with increase of the distance from the Fermi surface. This lowers somewhat the estimates of the EPI constant (see Ref. 36), whereas replacement of all the Γ_C vertices in (17) and (19) by Γ_C^0 and the use of relation (21) as the definition of Γ_C (see Ref. 21) overestimates the values of the coupling constant.

3. Using the spectral representation for the phonon Green's function $D_{ph}(q, \omega)$ and the Kramers-Kronig relation for the response function $\tilde{\epsilon}^{-1}(q, \omega)$, we reduce Eqs. (17) and (19), for weak damping in the region¹⁰⁾ $\omega \sim \omega_{max}$, under the condition

$$\tilde{\Omega}_+ \equiv \Omega_+(2k_{F1}) \ll \omega_{max}$$

to the standard Eliashberg equations⁷¹ for the renormalization gap parameter

$$\tilde{\Delta}_f(\omega) \equiv \Delta_f(\omega)/Z_f(\omega)$$

and the renormalization factor

$$Z_f(\omega) \equiv [1 - f_f(\omega)/\omega]$$

as $T \rightarrow T_c$:

$$\begin{aligned} Z_f(\omega) \tilde{\Delta}_f(\omega) = & \int_0^\infty \frac{d\omega'}{\omega'} \operatorname{Re} \tilde{\Delta}_f(\omega') [K_+^{pl}(\omega', \omega, T_c) \Gamma_C^0 \\ & + K_+^{ph}(\omega', \omega, T_c)] - \mu_C \int_0^{\tilde{E}_{F1}} \frac{d\omega'}{\omega'} \operatorname{Re} \tilde{\Delta}_f(\omega') \operatorname{th}(\omega'/2T_c) \Gamma_C^0, \end{aligned} \quad (22)$$

$$Z_f(\omega) = 1 - \frac{1}{\omega} \int_0^\infty d\omega' [K_-^{pl}(\omega', \omega, T_c) + K_-^{ph}(\omega', \omega, T_c)], \quad (23)$$

where

$$\begin{aligned} K_\pm^{pl, ph}(\omega', \omega, T_c) = & \frac{1}{2} \int_0^\infty d\omega'' [S_{pl}(\omega''), S_{ph}(\omega'')] \\ & \times \left[\operatorname{th} \left(\frac{\omega'}{2T_c} \right) + \operatorname{cth} \left(\frac{\omega''}{2T_c} \right) \right] \\ & \times \left(\frac{1}{\omega' + \omega'' + \omega + i\delta} \pm \frac{1}{\omega' + \omega'' - \omega - i\delta} \right) \\ & - \left[\operatorname{th} \left(\frac{\omega'}{2T_c} \right) - \operatorname{cth} \left(\frac{\omega''}{2T_c} \right) \right] \\ & \times \left(\frac{1}{\omega' - \omega'' + \omega + i\delta} \pm \frac{1}{\omega' - \omega'' - \omega - i\delta} \right), \end{aligned} \quad (24)$$

$$S_{ph}(\omega) = \tilde{v}_l \langle g_{ph}^2(\mathbf{q}) \rangle F_{ph}(\omega), \quad (25)$$

$$S_{pl}(\omega) = -\frac{1}{\pi} \tilde{v}_l \langle V_C(\mathbf{q}) \operatorname{Im} \tilde{\epsilon}^{-1}(\mathbf{q}, \omega) \rangle, \quad (26)$$

$$\mu_C = \tilde{v}_l \langle V_C(\mathbf{q}) \operatorname{Re} \tilde{\epsilon}^{-1}(\mathbf{q}, \omega_{max}) \rangle. \quad (27)$$

Here

$$\langle g_{ph}^2 \rangle \equiv \sum_j \langle g_j^2 \rangle$$

is the square of the EPI matrix element averaged over the FS, $F_{ph}(\omega)$ is the phonon density of states for those phonon modes which are not hybridized with acoustic plasmons and are described by the Green's function (16),

$$\tilde{v}_l(n) = v_l \beta(n)/c(n)$$

is the renormalized state density of the l -carriers on a cylindrical FS in a layered metal with n conducting layers per unit cell, and $\beta(n)$ is the corresponding structure factor of the normal and anomalous self-energy parts (see the Appendix and Fig. 3).

Note that the averaging over a weakly rippled cylindrical FS reduces approximately to integration over the transverse momentum p_z and over the azimuthal angle φ between \mathbf{p}_\parallel and \mathbf{p}'_\parallel . The latter can be replaced in the case of an isotropic (in the plane of the layers) electron spectrum by integration over the longitudinal momentum transfer $q_\parallel = |\mathbf{p}'_\parallel - \mathbf{p}_\parallel|$, and the Jacobian of the transition has a root singularity at the point $q_\parallel = 2k_{F1}$ (see Refs. 21 and 22).

In a real cuprate MOC crystal with initially isotropic spectrum and a wide $2D$ band (e.g., with a flattened congruent sections of the FS and the band almost half-filled, see Ref. 72), elastic scattering of the l -carriers by the lattice defects produce during the Cooper pairing almost effective isotropization (averaging over the angle φ) of both the quasiparticle spectrum and of the interaction between the quasiparticles, in accordance with the Anderson theorem⁷³ for "dirty" superconductors. Consequently the main contribution to the electron-phonon and electron-plasma interactions is made, just as in the isotropic case, by the region $q_\parallel \approx 2k_{F1}$.

As a result, with account taken of Eqs. (6) and (27), the dimensionless Coulomb repulsion constant can be estimated from the equation¹¹⁾

$$\mu_C(n) \cong \frac{\alpha_l}{2} \beta(n), \quad \alpha_l = \frac{m_l^* e^2}{\epsilon_\infty k_{Fl}} \cong \frac{1}{k_{Fl} a_l^*}, \quad (28)$$

where the quantity

$$\tilde{\epsilon}_\infty(q) = [\text{Re } \tilde{\epsilon}^{-1}(q, \omega_{max})]^{-1}$$

at $q_{||} = 2k_{Fl}$ can differ somewhat from the optical permittivity ϵ_∞ of the crystal as $q \rightarrow 0$.

4. From Eq. (23) under the condition $T_c \ll \min\{\tilde{\Omega}_+, \tilde{\omega}_{ph}\}$, where $\tilde{\omega}_{ph}$ is the average frequency of the phonons that hybridize with the acoustic plasmons, we obtain in the limit as $\omega \rightarrow 0$

$$Z_l(0) = 1 + \lambda_{ph} + \lambda_{pl}, \quad (29)$$

where

$$\lambda_{ph} = 2 \int_0^\infty \frac{d\omega}{\omega} S_{ph}(\omega), \quad \lambda_{pl} = 2 \int_0^\infty \frac{d\omega}{\omega} S_{pl}(\omega). \quad (30)$$

On the other hand, from Eq. (19) taking into account (4) with $\Gamma_C \approx 1$, which corresponds to the random phase approximation, we obtain in the limit as $\omega \rightarrow 0$ and $T \rightarrow 0$

$$f_{pl}(\omega) = -\tilde{v}_l \omega \int_0^{\omega_{max}} d\omega' \frac{\partial}{\partial \omega'} \langle D_{pl}(q, \omega') \rangle = -\omega(\mu_\infty - \mu_0), \quad (31)$$

where

$$\mu_\infty = \tilde{v}_l \langle V_C(q) \tilde{\epsilon}_\infty^{-1}(q) \rangle, \quad \mu_0 = \tilde{v}_l \langle V_C(q) \tilde{\epsilon}^{-1}(q, 0) \rangle. \quad (32)$$

Comparing (29) with (31) we see that the role of the electron-plasma interaction constant (by analogy with the electron-phonon interaction) is played by the quantity

$$\lambda_{pl} = \mu_\infty - \mu_0$$

(see Refs. 21, 22), and from Eq. (21) with taking into account Eq. (31), it follows that

$$\Gamma_C^0 = 1 + \lambda_{pl}$$

so that the effective coupling constant in (22) is equal to

$$\tilde{\lambda}_{pl} \cong \lambda_{pl}(1 + \lambda_{pl}).$$

Thus, in the case of predominant electron-plasma interaction ($\lambda_{pl} \gg \lambda_{ph}$), according to (21), (22), and (29), the non-adiabatic renormalization $Z_{pl}(0) = 1 + \lambda_{pl}$, of the interaction responsible for the Cooper pairing of the l -carriers is almost completely cancelled on the Fermi surface by the local-field corrections to the Coulomb vertex Γ_C , as noted earlier in Ref. 36 (see also Ref. 21).

Note that in crystal with high ionization, where¹²⁾ $\epsilon_0 \gg \epsilon_\infty$ and $\mu_0 \ll \mu_\infty$ we have with good accuracy $\lambda_{pl} \cong \mu_\infty \cong \mu_C$.

4. CRITICAL TEMPERATURE OF SC TRANSITION AND ISOTOPIC SHIFT INDEX T_c

Various approximate methods of solving the Eliashberg integral equations⁷¹ for superconductors with strong electron-phonon interactions have been previously considered in numerous studies (see the reviews, Refs. 29 and 68) with an aim at obtaining relatively simple analytic equations for the calculation of T_c . An empirical analysis and model calculations have shown (see, e.g., Refs. 74–79) that satisfactory results in the intermediate-coupling region ($\lambda_{ph} \lesssim 1$) are obtained with an exponential equation for T_c in the form

$$T_c = K \tilde{\omega}_{ph} \exp \left\{ - \frac{1 + \lambda_{ph}}{\lambda_{ph} - \mu_C^* (1 + L \lambda_{ph})} \right\}, \quad (33)$$

where μ_C^* is the Coulomb pseudopotential⁵³ and the parameters K and L depend on the form of the phonon spectrum and on the actual choice of the approximation, with $K < 1$ and $L < 1$ in all cases.

On the other hand, according to Ref. 80, in the case of strong coupling ($\lambda_{ph} \gg 1$) the equation for T_c should be

$$T_c \approx 0,18 \tilde{\omega}_{ph} \sqrt{\lambda_{ph}}, \quad (34)$$

which is valid, strictly, if $\pi T_c \gg \tilde{\omega}_{ph}$. Account must be taken here of the strong quasiparticle damping which was shown in Ref. 79 to lead to a “gapless” state with a complex gap parameter $\Delta(\omega)$ whose real and imaginary parts vanish on the FS and take as $\omega \rightarrow 0$ and $T \rightarrow T_c$ the form

$$\text{Re } \Delta(\omega) = \frac{\omega^2}{\gamma_{ph}^2} \Delta_0, \quad \text{Im } \Delta(\omega) = - \frac{\omega}{\gamma_{ph}} \Delta_1, \quad (35)$$

where Δ_0 and Δ_1 are certain constants, and $\gamma_{ph} \approx \lambda_{ph} T_c^3 / \tilde{\omega}_{ph}^2$ is the rate of the quasiparticle damping via inelastic relaxation on acoustic phonons.

2. In the framework of the considered model of layered two-band metal with predominant EPI and with a “plasmon” mechanism of Cooper pairing of degenerate l -carriers, the quasiparticle relaxation is mainly on virtual acoustic plasmons and is determined by their Landau damping on h -carriers (see Refs. 21 and 22). The damping decrement of the quasiparticles near the FS ($\omega \rightarrow 0$) in the normal state ($T \gg T_c$) is given by

$$\gamma_{pl}(T) = \pi \int_0^\infty \frac{S_{pl}(\omega) d\omega}{\text{sh}(\omega/2T) \text{ch}(\omega/2T)}. \quad (36)$$

In the case of nondegenerate almost localized h -carriers, γ_{pl} is an almost linear function of temperature in a wide T range. This explains, in particular, the nearly linear T -dependence of the resistance of cuprate MOC.^{54,55}

In the region $\omega \ll \tilde{\Omega}_+$, $\tilde{\omega}_{ph}$ it follows from (22) and (23) that

$$\text{Re}[Z_l(\omega) \tilde{\Delta}_l(\omega)] = C_1, \quad \text{Im}[Z_l(\omega) \tilde{\Delta}_l(\omega)] = \omega C_2, \quad (37)$$

$$\text{Re } Z_l(\omega) \cong 1 + \lambda, \quad \text{Im } Z_l(\omega) = \gamma_l / \omega, \quad (38)$$

where $\lambda = \lambda_{ph} + \lambda_{pl}$ and $\gamma_l = \gamma_{ph} + \gamma_{pl}$, while $C_{1,2}$ are quantities that depend little on ω (see Ref. 79). Hence

$$\operatorname{Re} \tilde{\Delta}_l(\omega) = \frac{\omega^2 \Delta_0}{\gamma_l^2 + \omega^2(1 + \lambda)^2}, \quad \Delta_0 = (1 + \lambda)C_1 + \gamma_l C_2,$$

$$\operatorname{Im} \tilde{\Delta}_l(\omega) = -\frac{\omega}{\gamma_l} \frac{\gamma_l^2 \Delta_1 - \omega^2(1 + \lambda)[\Delta_0 - (1 + \lambda)\Delta_1]}{\gamma_l^2 + \omega^2(1 + \lambda)^2},$$
(39)

$$\Delta_1 = C_1. \quad (40)$$

From the dispersion equation for $\tilde{\Delta}_l(\omega)$ (Ref. 81), as $\omega \rightarrow 0$ and $T \rightarrow T_c$,

$$\left[\frac{\operatorname{Im} \tilde{\Delta}_l(\omega)}{\omega} \right]_{\omega=0} = -\frac{2}{\pi} \int_0^{\infty} \frac{dz}{z^2} \operatorname{Re} \tilde{\Delta}_l(z) \quad (41)$$

we obtain, taking (39) and (40) into account, the connection between the parameters Δ_0 and Δ_1 :

$$\Delta_0 = \Delta_1(1 + \lambda). \quad (42)$$

It follows from (39) and (22) that the presence of "gapless" region near the FS at

$$\omega < \tilde{\gamma}_l = \gamma_l/(1 + \lambda)$$

must be taken into account in the calculation of T_c if the condition $\tilde{\gamma}_l \gtrsim T_c$ is satisfied. In the case of a strong electron-phonon interaction ($\lambda_{ph} \gg 1$) this condition reduces to the inequality $T_c \gtrsim \tilde{\omega}_{ph}$, i.e., corresponds in fact to the condition that Eq. (34) be valid.

3. For an approximate solution of Eq. (22) we approximate $\operatorname{Re} \tilde{\Delta}_l(\omega)$ in the integrands, with allowance for (39), by an alternating-sign step function (cf. Refs. 74 and 76):

$$\operatorname{Re} \tilde{\Delta}_l(\omega) = \frac{\omega^2 \tilde{\Delta}_0}{\tilde{\gamma}_l^2 + \omega^2} \theta(\tilde{\omega}_0 - \omega) - \Delta_{\infty} \theta(\omega - \tilde{\omega}_0) \theta(E_{Fl} - \omega),$$
(43)

where $\tilde{\Delta}_0 = \Delta_0/(1 + \lambda)^2$, and the frequency $\tilde{\omega}_0$ is determined from the condition

$$\operatorname{Re} \tilde{\Delta}_l(\tilde{\omega}_0) = 0$$

(see below).

Substituting (43) in (22) we easily verify that if $T_c < \tilde{\gamma}_l$ the Cooper logarithm has a lower cutoff limit $\tilde{\gamma}_l$, so that T_c depends on the character of the temperature dependence of the decrement $\gamma_l(T)$ of the damping of quasiparticles by virtual acoustic phonons and acoustic plasmons as $T \rightarrow T_c$ [see (36)].

On the other hand, if $T_c > \tilde{\gamma}_l$ (but $T_c \ll \tilde{\Omega}_+, \tilde{\omega}_{ph}$), the "zero gap" region ($\omega \lesssim \tilde{\gamma}_l$) can be neglected¹³⁾ and T_c can be calculating using a previously obtained⁷⁶⁾ approximate exponential equation having, with allowance for (42) and the local-field corrections (21) the form

$$T_c = \tilde{\omega}_0 \exp \left\{ -\frac{1 + \lambda + \tilde{\lambda}_0(\tilde{\omega}_0)}{\tilde{\lambda} - \tilde{\mu}_C^*(\tilde{\omega}_0)[1 + \tilde{\lambda}_{\infty}(\tilde{\omega}_0)]} \right\}, \quad (44)$$

where

$$\tilde{\lambda} = \lambda_{ph} + \lambda_{pl}, \quad \tilde{\lambda} = \lambda_{ph} + \tilde{\lambda}_{pl}, \quad \tilde{\lambda}_{pl} = \lambda_{pl}(1 + \lambda_{pl}),$$
(45)

$$\tilde{\lambda}_0(\tilde{\omega}_0) = 2 \int_0^{\infty} \frac{d\omega}{\omega} [S_{ph}(\omega) + (1 + \lambda_{pl})S_{pl}(\omega)] \ln \left(1 + \frac{\tilde{\omega}_0}{\omega} \right),$$
(46)

$$\tilde{\lambda}_{\infty}(\tilde{\omega}_0) = 2 \int_0^{\infty} \frac{d\omega}{\omega} [S_{ph}(\omega) + (1 + \lambda_{pl})S_{pl}(\omega)] \ln \left(1 + \frac{\omega}{\tilde{\omega}_0} \right).$$
(47)

$$\tilde{\mu}_C^*(\tilde{\omega}_0) = \tilde{\mu}_C [1 + \tilde{\mu}_C \ln(E_{Fl}/\tilde{\omega}_0)]^{-1}, \quad \tilde{\mu}_C = \mu_C(1 + \lambda_{pl}).$$
(48)

To estimate T_c and to analyze the dependences of T_c on various parameters, we begin with the Einstein model of a spectrum with two δ -function peaks:

$$\tilde{S}(\omega) = \frac{\lambda_{ph}}{2} \Omega_0 \delta(\omega - \Omega_0) + \frac{\tilde{\lambda}_{pl}}{2} \tilde{\Omega}_+ \delta(\omega - \tilde{\Omega}_+), \quad (49)$$

where Ω_0 is the frequency of the hf dipole-active (polar) optical mode corresponding to oxygen-ion oscillations in dielectric oxide layers and appears in the Raman spectra of cuprate MOC in ω_{xx} polarization transverse to the plane of the layers,^{19,20} while $\tilde{\Omega}_+$ is the frequency of the hybrid phonon-plasma oscillations (11) at $q_{\parallel} = 2k_{Fl}$ and $\omega_{LO} \gg \omega_{TO}$:

$$\tilde{\Omega}_+(n) = \left[\frac{\Omega_h^2 \tilde{\beta}(n) k_{Fl} d + \omega_{LO}^2}{1 + \alpha_l \tilde{\beta}(n)} \right]^{1/2}. \quad (50)$$

Note that the frequency of the lf optical mode ω_{LO} , which corresponds to oxygen-ion oscillations in CuO_2 layers, should be observed in a longitudinal polarization $\omega_{xx} = \omega_{xy} = \omega_{yy}$ in the Raman spectra of nonsuperconducting (dielectric) phases of the cuprate MOC,¹⁴⁾ whereas a higher hybrid mode Ω_+ is apparently observed in metallic superconducting phases.^{19,20}

The parameters $\tilde{\lambda}_0$ and $\tilde{\lambda}_{\infty}$ for the spectrum (49) take according to (45) and (46) the form

$$\tilde{\lambda}_0(\tilde{\omega}_0) = \lambda_{ph} \ln \left(1 + \frac{\tilde{\omega}_0}{\Omega_0} \right) + \tilde{\lambda}_{pl} \ln \left(1 + \frac{\tilde{\omega}_0}{\tilde{\Omega}_+} \right), \quad (51)$$

$$\tilde{\lambda}_{\infty}(\tilde{\omega}_0) = \lambda_{ph} \ln \left(1 + \frac{\Omega_0}{\tilde{\omega}_0} \right) + \tilde{\lambda}_{pl} \ln \left(1 + \frac{\tilde{\Omega}_+}{\tilde{\omega}_0} \right), \quad (52)$$

while the frequency $\tilde{\omega}_0$ is determined, according to (22) and (24), with allowance for (37)–(43), by the equation (cf. Ref. 76):

$$\frac{\tilde{\gamma}_l^2 \tilde{\Delta}_1}{\tilde{\omega}_0^2 + \tilde{\gamma}_l^2} = \tilde{\Delta}_0 \int_0^{\tilde{\omega}_0} \frac{\omega d\omega}{\omega^2 + \tilde{\gamma}_l^2} \left[\tilde{K}_+(\omega, \tilde{\omega}_0, T_c) - \tilde{\mu}_C^*(\tilde{\omega}_0) \text{th} \left(\frac{\omega}{2T_c} \right) \right], \quad (53)$$

where

$$\tilde{\Delta}_1 = \Delta_1 / (1 + \lambda) \equiv \tilde{\Delta}_0.$$

Under the condition

$$\tilde{\gamma}_l \leq T_c \ll \tilde{\Omega}_+, \Omega_0$$

we can put in (53), with good accuracy,

$$\tilde{K}_+(\omega, \tilde{\omega}_0, T_c) \approx \text{th} \left(\frac{\omega}{2T_c} \right) \left[\frac{\lambda_{ph} \Omega_0^2}{\Omega_0^2 - \tilde{\omega}_0^2} + \frac{\tilde{\lambda}_{pl} \tilde{\Omega}_+^2}{\tilde{\Omega}_+^2 - \tilde{\omega}_0^2} \right]. \quad (54)$$

This yields at $\tilde{\gamma}_l \ll \tilde{\omega}_0$ and $\tilde{\mu}_C^* \ll \tilde{\lambda}$

$$\tilde{\omega}_0 \equiv \Omega_0 \tilde{\Omega}_+ / \langle \omega^2 \rangle^{1/2}, \quad (55)$$

where

$$\langle \omega^2 \rangle \equiv \frac{2}{\tilde{\lambda}} \int_0^{\tilde{\omega}_0} \omega d\omega \tilde{S}(\omega) = \frac{1}{\tilde{\lambda}} (\lambda_{ph} \Omega_0^2 + \tilde{\lambda}_{pl} \tilde{\Omega}_+^2). \quad (56)$$

Note that expressions (55) and (56) yield satisfactory results and comparable values of the electron-phonon and electron-polaron interaction constants ($\lambda_{ph} \sim \tilde{\lambda}_{pl}$), whereas as $\lambda_{ph} \rightarrow 0$ or $\lambda_{pl} \rightarrow 0$ Eqs. (55) and (56) lead to the incorrect limiting values $\tilde{\omega}_0 = \Omega_0$ or $\tilde{\omega}_0 = \tilde{\Omega}_+$, thus pointing to the need for a more logical self-consistent definition of the point where $\text{Re } \Delta_l(\omega)$ reverses sign (see Refs. 76 and 77). We therefore choose $\tilde{\omega}_0$ to be the rms spectrum frequency, which is defined by (56) and which leads as $\lambda_{ph} \rightarrow 0$ and $\lambda_{pl} \rightarrow 0$ to the correct limiting values $\langle \omega^2 \rangle^{1/2} = \tilde{\Omega}_+$ or $\langle \omega^2 \rangle^{1/2} = \Omega_0$.

4. From (44), taking (50) and (56) into account, we obtain for the oxygen isotopic-effect index¹⁵⁾

$$\alpha_O \equiv - \frac{\partial \ln T_c}{\partial \ln M_O} \equiv \frac{1}{2\tilde{\lambda}\tilde{\omega}_0^2} \left[\lambda_{ph} \Omega_0^2 + \frac{\tilde{\lambda}_{pl} \omega_{LO}^2}{1 + \alpha_l \beta(n)} \right] \times \left\{ 1 - \frac{1 + \tilde{\lambda}_\infty(\tilde{\omega}_0)}{1 + \lambda_{ph} + \lambda_{pl} + \tilde{\lambda}_0(\tilde{\omega}_0)} \left[\frac{\tilde{\mu}_C^*(\tilde{\omega}_0)}{\Lambda(\tilde{\omega}_0)} \right]^2 \right\}, \quad (57)$$

where

$$\Lambda(\tilde{\omega}_0) = \frac{\lambda_{ph} + \tilde{\lambda}_{pl} - \tilde{\mu}_C^*(\tilde{\omega}_0) [1 + \tilde{\lambda}_\infty(\tilde{\omega}_0)]}{1 + \lambda_{ph} + \lambda_{pl} + \tilde{\lambda}_0(\tilde{\omega}_0)}. \quad (58)$$

Since

$$\Omega_0^2 \gg \omega_{LO}^2 [1 + \alpha_l \beta(n)]^{-1},$$

the value of α_0 depends substantially on the electron-phonon interaction constant even when $\lambda_{ph} \ll \tilde{\lambda}_{pl}$. We assume hereafter that the polar electron-phonon interaction effect with an hf oxygen mode Ω_0 (just as with an lf mode ω_{LO}) is based on a Coulomb interaction of l -carriers localized in 2D layers of CuO_2 , with the oxygen ions located outside the cuprate layers in a region with lower electron density.¹⁶⁾ We therefore put $\lambda_{ph} = \kappa \tilde{\lambda}_{pl}$ in the numerator of (58), as well as in (51) and (52), whenever λ_{ph} plays the role of the interelectron attraction constant, and put $\lambda_{ph} = \kappa \lambda_{pl}$ in the denominator of (58) when λ_{ph} determines the renormalization of Λ by the electron-phonon interaction. The dimensionless parameter $\kappa < 1$ is indicative of the degree of attenuation of the polar electron-phonon interaction with vibrational modes of the oxygen outside the planes (more follows).

With λ_{ph} so defined, an appreciable part of the renormalizations of the effective coupling constant Λ due to electron-plasmon and electron-phonon interaction by the local field corrections [see (21)], so that if $\lambda_{pl} \equiv \mu_c$ and $\tilde{\lambda}_{pl} \equiv \mu_c (1 + \mu_c)$ expression (58) can be written in the form

$$\Lambda \equiv \frac{\mu_c (1 + \kappa) - \mu_c^* (1 + \tilde{\lambda}_\infty)}{1 + \kappa \mu_c + \lambda_0}, \quad (59)$$

where

$$\lambda_0 = \tilde{\lambda}_0 / (1 + \mu_c)$$

and

$$\mu_c^* = \tilde{\mu}_C^* / (1 + \mu_c).$$

Thus, the electron-plasmon and polar electron-phonon interactions are considerably enhanced by the multiparticle correlation effects in the Coulomb interaction (see Refs. 21, 36, 43).

Note that there is no such cancellation of the renormalization (and a corresponding enhancement of the interaction) in the case of nonpolar electron-phonon interaction, and the electron-phonon interaction constant for a multilayer structure with n conducting CuO_2 layers per packet (Fig. 2) contains an additional factor $\beta(n) d/c(n)$, and consequently increases with increase of n much more slowly than the electron-polaron interaction $\lambda_{pl}(n) \approx \mu_c(n) \sim \beta(n)$.

5. COMPARISON OF THEORY WITH EXPERIMENT

1. To analyze the results and to compare them with the experimental data on HTSC in cuprate MOC, we shall estimate some realistic values of the model parameters. We estimate first the longitudinal effective mass of the l -carriers in a wide 2D band, starting with calculated and empirical data on the width of the cuprate-MOC hybrid pd band located in the interval $W_l \approx 1-4$ eV, corresponding at a ≈ 4 Å to values

$$m_l^* = 4/a^2 W_l \approx (0.5 - 2) m_0,$$

where m_0 is the free-electron mass.

The 2D l -carrier density N_l per unit cuprate-layer area in layered MOC with n conducting CuO_2 layers per unit cell, gathered into packets of thickness

$$L(n) = (n - 1)d_0$$

(see Fig. 2), with the electrons (holes) uniformly distributed among the layers in the packet, is connected with the average l -carrier bulk density \bar{n}_l by the relation

$$N_l(n) = \bar{n}_l c(n)/n, \quad c(n) = d + L(n). \quad (60)$$

When the number of CuO_2 layers in the packet is increased, the number of x_l l -carriers in the primitive-cell volume,

$$v_0(n) = abc(n),$$

can be conserved ($x_l = \text{const}$) if it is determined by a fixed number of atoms of the non-isovalent impurity with constant valency. In this case the density \bar{n}_l , the $2D$ density N_l , the Fermi momentum $k_{F1} = \sqrt{2\pi N_l}$, and the Fermi energy $E_{F1} = k_{F1}^2/2m_l^*$ of the degenerate l -carriers in the CuO_2 layers all decrease, and their dimensionless density parameter

$$\alpha_l = 1/k_{F1} a_l^*$$

increases with increase of n in accordance with the relation (for $a = b$):

$$\begin{aligned} \bar{n}_l(n) &= \frac{x_l}{a^2 c(n)}, & N_l(n) &= \frac{x_l}{a^2 n}, & k_{F1}(n) &= \frac{1}{a} \sqrt{\frac{2\pi x_l}{n}}, \\ \bar{E}_{F1}(n) &= \frac{\pi x_l}{m_l^* a^2 n}, & \alpha_l(n) &= \frac{a}{a_l^*} \sqrt{\frac{n}{2\pi x_l}}. \end{aligned} \quad (61)$$

Experiment,^{57,82-84} however, shows that in most cuprate MOC the plasma frequency of the majority carriers depends little on the number of CuO_2 layers in the unit cell. Thus, for example in the compounds $\text{Bi}_2\text{Sr}_2\text{CaCu}_2\text{O}_8$ with $n = 2$ and $\text{Tl}_2\text{Ba}_2\text{Ca}_2\text{Cu}_3\text{O}_{10}$ with $n = 3$ the longitudinal (in the layer plane) plasma frequency is equal to $\omega_{pl}'' \approx 1.1-1.2$ eV (Ref. 83), and in $\text{YBa}_2\text{Cu}_3\text{O}_7$ it is somewhat lower ($\omega_{pl}'' \approx 1.4$ eV). Here, however, there are in addition to the CuO_2 $2D$ -layers also $1D$ CuO chains whose contribution can be substantial (see Ref. 57).

Thus, if it is assumed that when the number of cuprate CuO_2 layers is increased the bulk density of the l -carriers remains almost constant ($\bar{n}_l \approx \text{const}$), for example on account of the variable valencies of the Bi and Tl ions or on account of the excess oxygen, we obtain according to (60)

$$\begin{aligned} N_l(n) &= \frac{\tilde{x}_l^2}{2\pi a^2} \frac{\delta_0 + n - 1}{n}, & k_{F1}(n) &= \frac{\tilde{x}_l}{a} \sqrt{\frac{\delta_0 + n - 1}{n}}, \\ \bar{E}_{F1}(n) &= \frac{\tilde{x}_l^2}{2m_l^* a^2} \frac{\delta_0 + n - 1}{n}, & \alpha_l(n) &= \frac{a}{a_l^* \tilde{x}_l} \sqrt{\frac{n}{\delta_0 + n - 1}}, \end{aligned} \quad (62)$$

$$\tilde{x}_l = (2\pi \bar{n}_l a^2 d_0)^{1/2}, \quad \delta_0 = d/d_0. \quad (63)$$

On the other hand, the effective l -carrier mass can be estimated from the experimental values $\omega_{pl}'' \approx 1.4-1.5$ eV and

$\varepsilon_\infty \approx 3.8-5.2$ for $\text{YBa}_2\text{Cu}_3\text{O}_7$ (Refs. 82, 83) at a hole density $\bar{n}_p \approx 5.8 \cdot 10^{21} \text{ cm}^{-3}$, which corresponds to one extra hole per unit-cell volume (according to the chemical valencies of the components). Assuming that the longitudinal effective masses and densities of the holes in the $2D$ -layers of CuO_2 and $1D$ -chains of CuO are approximately equal (see Ref. 57), we obtain for the l -carrier band effective mass and for the band width the respective estimates $m_B^* \approx (0.7-1.1)m_0$ and $W_l \approx (1.8-2.9)$ eV.

It must be taken into account at the same time that the definitions of \bar{E}_{F1} and α_l in (61) and (62) contain the quasiparticle effective mass renormalized to multiparticle correlations

$$m_l^* = m_B^* [1 - 2m_B \Sigma_C(k_{F1}, 0)/k_{F1}^2]^{-1}, \quad (64)$$

which can be considerably larger than the optical (band) mass m_B^* .

2. As noted above, the effective h -carrier mass $m_h^* = 4/a^2 W_h$ of the h -carriers in a narrow $2D$ band of width $W_h \ll W_l$ can be increased by polaron effects, which are manifested also under conditions of screening by l -carriers (see Ref. 65). Since m_h^* is unknown, we use hereafter, as the parameter that depends on the h -carrier density, the square of the ratio of their plasma frequency and the LO-phonon frequency, contained in the expression for the frequency of hybrid phonon-plasma oscillations [see (50)]:

$$\tilde{\Omega}_+(n) = \omega_{LO} \left[\frac{\tilde{x}_h \tilde{\beta}(n) \tilde{k}_{F1}(n) + 1}{\alpha_l(n) \tilde{\beta}(n) + 1} \right]^{1/2}, \quad (65)$$

where

$$\tilde{x}_h = \frac{\tilde{\Omega}_h^2}{\omega_{LO}^2} \equiv \frac{4\pi e^2 \tilde{N}_h}{\varepsilon_\infty m_h^* a \omega_{LO}^2}, \quad \tilde{k}_{F1}(n) \equiv k_{F1}(n)a. \quad (66)$$

Here \tilde{N}_h is the effective $2D$ density of the h -carriers in a narrow band.

It is assumed in the considered band-spectrum model that at the point of dielectric-metal phase transition the FS of the degenerate l -carriers is "pinned" on the edge of the narrow $2D$ band ($\bar{E}_{F1} = E_0$) with high density of states ($v_h \gg \tilde{v}_l$), and the subsequent doping increases mainly the density \tilde{N}_h of the h -carriers, whereas the l -carrier density remains almost constant ($N_l \approx \text{const}$).

3. Equations (44), (45), (50)-(52) and (56) with allowance for relations (60)-(63) and (65), were used to calculate the dependences of T_c on $\tilde{x}_h \equiv (\tilde{\Omega}_h/\omega_{LO})^2$, for various $n = 1-5$ at $\lambda_{pl}(n) = \mu_c(n) = \alpha_l(n)\tilde{\beta}(n)/2$ and $\lambda_{ph} = \kappa \lambda_{pl}(n)$ or $\lambda_{ph} = \kappa \tilde{\lambda}_{pl}(n)$, where the parameter κ was estimated from tunnel-spectroscopy data⁴⁶ as the ratio of the areas of the lf and hf peaks with weight ω^{-1} ($\kappa \leq 0.3$).

Figure 4 shows the dependences of T_c on \tilde{x}_h for the parameter values $d = 12$ Å, $d_0 = 3.2$ Å, $a = 3.9$ Å, $\omega_{LO} = \omega_{xx} = 300$ K and $\Omega_0 = \omega_{zz} = 900$ K, corresponding to multilayer cuprate MOC of the type $\text{Bi}_2\text{Sr}_2\text{Ca}_{n-1}\text{Cu}_n\text{O}_x$ and $\text{Tl}_2\text{Ba}_2\text{Ca}_{n-1}\text{Cu}_n\text{O}_x$. We see that it is possible to obtain satisfactory qualitative and quantitative agreement between theory and experiment, particularly a maximum value $T_c^{\text{max}} \approx 125$ K close to experimental at $n = 3$.

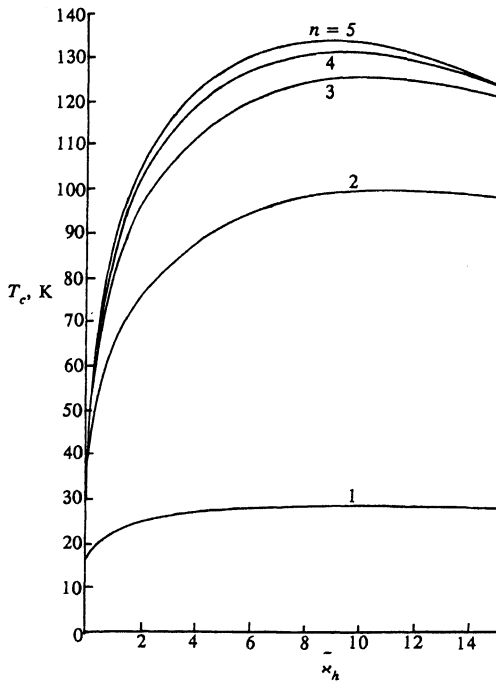


FIG. 4. Dependences of T_c on $\tilde{\kappa}_h = \tilde{\Omega}_h^2/\omega_{LO}^2$ for various n at $d/d_0 \equiv \delta = 3.75$, $\varepsilon_\infty = 4$, $\kappa = 0.2$, $\omega_{LO} = 300$ K, $\Omega_0 = 900$ K, $m_l^* = 1.8m_0$, $\kappa_l = 1.1$, corresponding to $Tl_2Ba_2Ca_{n-1}Cu_nO_x$ ($T_c^{\max} \approx 125$ K at $n = 3$) for $n_l = 4.3 \cdot 10^{21}$ cm $^{-3}$. (The curves with $n = 4$ and 5 pertain to hypothetical compounds of this class).

Figure 5 shows the dependences of the effective coupling constant Λ (59) and of the effective Coulomb pseudopotential $\tilde{\mu}_c^*$ (48) on $\tilde{\kappa}_h$, while Fig. 6 shows the functions $\tilde{\Omega}_+$ (65) and $\tilde{\omega}_0 = \langle \omega^2 \rangle^{1/2}$ (56), corresponding to the parameters of Fig. 4. It follows hence that the nonmonotonic dependence of T_c on $\tilde{\kappa}_h$ (i.e., on y_0 or x_d), within the framework of the considered model of the "plasmon" HTSC

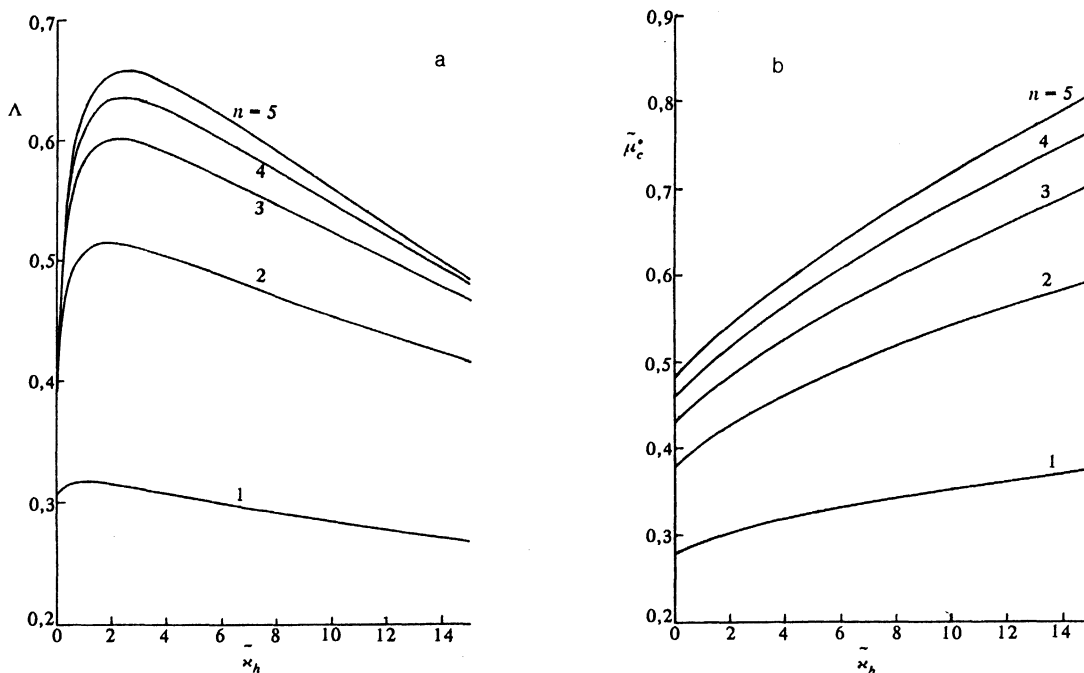


FIG. 5. Dependences of Ω (a) and $\tilde{\mu}_c^*$ (b) on $\tilde{\kappa}_h$ for various n (with the same parameters and values of n as in Fig. 4).

mechanism, is due to competition between two effects: expansion of the region of the effective interelectron attraction, due to the increase of the frequency of the hybrid phonon-plasma oscillations $\tilde{\Omega}_+$ (Fig. 6a) and consequently the average frequency $\tilde{\omega}_0$ of the spectrum (Fig. 6b), on the one hand, and the enhancement of the Coulomb repulsion on account of the decrease of the Bogolyubov-Tolmachev logarithm $\ln(\tilde{E}_{FI}/\tilde{\omega}_0)$ in the Morel-Anderson pseudopotential $\tilde{\mu}_c^*$ (Fig. 5b), which makes Λ nonmonotonic (Fig. 5a).

Note that the relation

$$T_c^{\max} \approx \tilde{\Omega}_+^{\max}/2\pi, \quad (Z)$$

which is indicative of the single-mode models⁴⁹ is satisfied with good accuracy for the maximum value of T_c at $n = 3$ in Fig. 4 and for the corresponding hybrid frequency $\tilde{\Omega}_+^{\max} \approx 795$ K. This attests to predominant role of the hybrid mode of the phonon-plasma oscillations Ω_+ (q) in Cooper pairing of l -carriers.

4. Figure 7 shows those dependences of T_c on $\tilde{\kappa}_h$ which have been obtained for the same parameters but at $d = 9.6$ Å ($\delta = 3$), corresponding to a layered MOC of the type $TlBa_2Ca_{n-1}Cu_nO_x$ with a TlO monolayer, for different values of n . These agree well with experiment.^{16,17} The most characteristic feature of this compound, observed in experiment and obtained theoretically on the basis of the considered model, is inversion of the lowering of the T_c ($\tilde{\kappa}_h$) curve at $n > 3$ with $T_c^{\max} \approx 110$ K at $n = 3$.

Figure 8 shows the dependence of T_c^{\max} on n for the parameters of Fig. 7. It is seen that T_c^{\max} is a nonmonotonic function of the number of the CuO_2 cuprate layers in the unit cell of the multilayer compound $TlBa_2Ca_{n-1}Cu_nO_x$ (Ref. 18) shows also plots of $T_c^{\max}(n)$ corresponding to the parameters of Fig. 4 for $Tl_2Ba_2Ca_{n-1}Cu_nO_x$ (and also for $Bi_2Sr_2Ca_{n-1}Cu_nO_x$) and demonstrating the deviation from the "chew rule" (tendency of T_c to saturate with increase of n) in multilayer cuprate MOC.

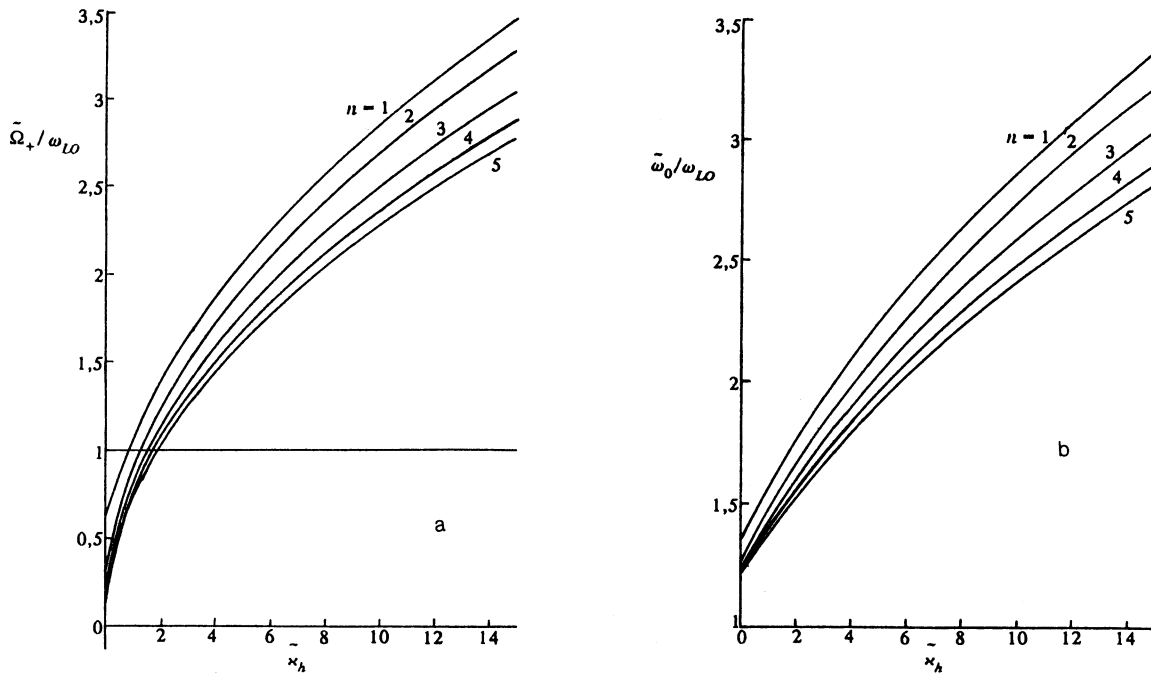


FIG. 6. Dependences of $\tilde{\Omega}_+$ (a) and $\tilde{\omega}_0$ (b) on $\tilde{\kappa}_h$ for various n (at the same parameters and values of n as in Fig. 4).

Such an n -dependence of T_c^{\max} , which agrees with experiment, is due in this model to the decrease of the Fermi momentum $k_{\text{F1}}(n)$ with increase of n [see Eq. (62)], whereby the parameter $\alpha_l(n) \sim k_{\text{F1}}^{-1}(n)$ increases while the quantities $\tilde{E}_{\text{F1}}(n) \sim k_{\text{F1}}^2(n)$, $\tilde{\Omega}_+(n)$ and $\tilde{\omega}_0(n)$ decreases (see Figs. 6a,b), with $\tilde{E}_{\text{F1}}(n)$ decreasing much faster than $\tilde{\omega}_0(n)$, so that the Coulomb pseudopotential $\tilde{\mu}_c^*(n)$ increases with n (Fig. 5b). As a result, the increase of the EPI constant

$\lambda_{\text{pl}}(n) \approx \alpha_l(n)\beta(n)/2$ with increase of n in the region of the saturation of the exponential in (44) is offset by the decrease of the pre-exponential factor $\tilde{\omega}_0(n)$ and by the increase of $\tilde{\mu}_c^*(n)$ due to the decrease of the ratio $\tilde{E}_{\text{F1}}(n)/\tilde{\omega}_0(n)$.

On the other hand, the increase of the distance d between the packets of the alternating CuO_2 and Ca layers (i.e., of the dimensionless parameter $\delta_0 \equiv d/d_0$) leads, according to (62), to an increase of k_{F1} , i.e., to a decrease of the parameter $\alpha_l \sim k_{\text{F1}}^{-1}$, but on the other hand to a faster increase of $\tilde{E}_{\text{F1}} \sim k_{\text{F1}}^2$, which is accompanied by a weakening of the Coulomb repulsion (a decrease of $\tilde{\mu}_c^*$) and an increase of

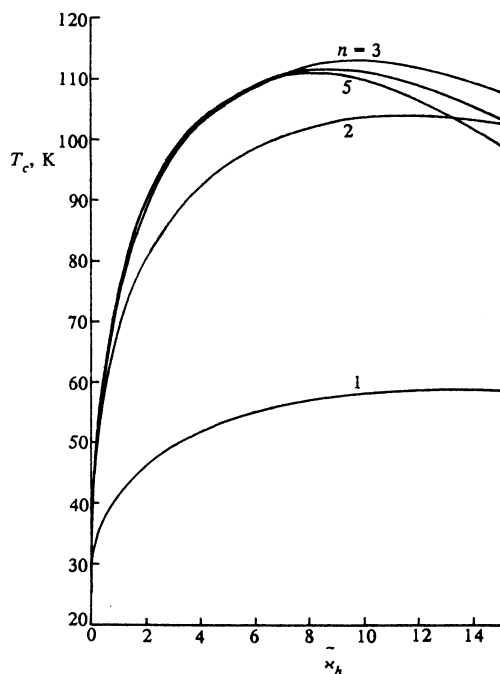


FIG. 7. Dependences of T_c on $\tilde{\kappa}_h$ for $n = (1-5)$ at $\delta = 3$, $\epsilon_\infty = 4$, $\kappa = 0.2$, $m^* = 1.8m_0$, $\kappa_l = 1.1$, $\Omega_0/\omega_{\text{LO}} = 3$, $\omega_{\text{LO}} = 300$ K, corresponding to $\text{TlBa}_2\text{Ca}_{n-1}\text{Cu}_n\text{O}_x$ with $T_c^{\max} \approx 110$ K for $n = 3$ (the notation is the same as in Fig. 4).

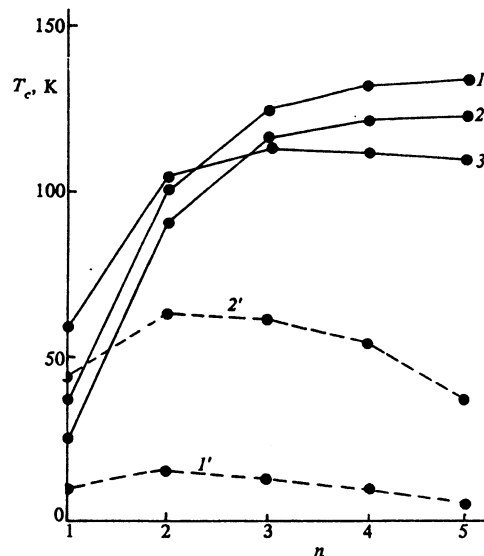


FIG. 8. Dependences of T_c^{\max} on n for EPI and polar EPHI in MOC layers of type $\text{Tl}_2\text{Ba}_2\text{Ca}_{n-1}\text{Cu}_n\text{O}_x$ (Fig. 4) and $\text{TlBa}_2\text{Ca}_{n-1}\text{Cu}_n\text{O}_x$ (Fig. 7)—solid curves 1 and 3, respectively, and also for $\text{Bi}_2\text{Sr}_2\text{Ca}_{n-1}\text{Cu}_n\text{O}_x$ with $T_c^{\max} = 115$ K for $n = 3$ ($m^* = 1.6m_0$, $\tilde{\kappa}_l = 1$, $\epsilon_\infty = \delta_0 = 3$)—curve 2. Dashed curve—plots of T_c vs n for nonpolar EPHI with $\lambda_{\text{ph}}(1) = 1$ (curve 1) and $\lambda_{\text{ph}}(1) = 2$ (curve 2) for $\lambda_{\text{ph}}(n) = \lambda_{\text{ph}}(1)\beta(n), d/c(n)$.

T_c in the region of the maximum, where the dependence of T_c on α_l is relatively weak. This explains the somewhat higher values of T_c^{\max} in bismuth and thallium MOC with BiO and TlO bilayers (Fig. 4) compared with T_c^{\max} in thallium MOC with TlO monolayers (Fig. 7).

The dashed lines of Fig. 8 show the dependences of T_c on n in the case of a predominant nonpolar electron-phonon interaction, when the coupling constant is

$$\lambda_{ph}(n) = \lambda_{ph}(1)\beta(n)d/c(n). \quad (\text{AE})$$

We see that these dependences differ greatly from the corresponding ones in the case of EPI with a coupling constant

$$\Lambda_\infty = \frac{(1 + \kappa) \ln(\tilde{E}_{F1}^\infty / \tilde{\omega}_0^\infty) - [\kappa \ln(1 + \Omega_0 / \tilde{\omega}_0^\infty) + \ln(1 + \tilde{\Omega}_+^\infty / \tilde{\omega}_0^\infty)]}{\ln(\tilde{E}_{F1}^\infty / \tilde{\omega}_0^\infty) [\kappa \ln(1 + \omega_0^\infty / \Omega_0) + \ln(1 + \omega_0^\infty / \tilde{\Omega}_+^\infty)]}, \quad (67)$$

where

$$\tilde{\omega}_0^\infty = \frac{1}{\sqrt{1 + \kappa}} [\kappa \Omega_0^2 + (\tilde{\Omega}_+^\infty)^2]^{1/2}, \quad \tilde{E}_{F1}^\infty = \frac{(k_{F1}^\infty)^2}{2m_l^*}, \quad (68)$$

$$\tilde{\Omega}_+^\infty = \tilde{\Omega}_h \sqrt{\frac{k_{F1}^\infty d}{\alpha_l}}, \quad \alpha_l^\infty = \frac{1}{k_{F1}^\infty d_l}, \quad k_{F1}^\infty = (2\pi \bar{n}_l d_0)^{1/2}. \quad (69)$$

T_c reaches then its limiting value (for $\Lambda_\infty > 0$)

$$T_c^\infty = \tilde{\omega}_0^\infty \exp(-1/\Lambda_\infty), \quad (70)$$

which depends on the parameters and can be high enough at $\tilde{E}_{F1} \gg \tilde{\omega}_0^\infty$. In particular, for the parameters of Fig. 4, when the effective mass decreases from the value $m_l^* = 1.8m_0$ to $m_l^* = m_0$ the value of T_c^∞ increases, according to (67)–(70), from 100 to 180 K.

Since the compound $(\text{Ca}_{1-x}\text{Sr}_x)_{1-y}\text{CuO}_2$ with an "infinite" number of cuprate layers corresponds to stoichiometric composition ($x = y = 0$) to a simple layered crystal with one CuO_2 layer per unit cell, it might seem that, by analogy with $\text{La}_{2-x}(\text{Ba}, \text{Sr})_x\text{CuO}_4$ or $\text{Bi}_2\text{Sr}_2\text{CuO}_x$, it should have a low $T_c \lesssim 20$ –40 K. However, the proximity of the CuO_2 superconducting layers, with distances $d_c \approx 3 \text{ \AA}$ between them comparable to the transverse coherence length⁸⁵ $\xi_\perp = \xi_\parallel \sqrt{m_\parallel^*/m_\perp^*}$,⁸⁵ contributes to a rise of T_c , in contrast to lanthanum or bismuth MOC with $n = 1$, in which single superconducting CuO_2 layers are much farther spaced, $d \approx 6$ –12 \AA apart, and the coupling between is weaker (of the Josephson type).

6. Assuming that near the Fermi level there is no narrow 2D band partly filled with h -carriers ($\tilde{N}_h = 0$ and $\tilde{\Omega}_h = 0$), thereby excluding the EPI and retaining only the polar electron-phonon interaction with oxygen optical modes ω_{LO} and Ω_0 (with the same coupling constant λ_{pl}), the maximum values of T_c are drastically decreased and the dependence of T_c on the carrier density and on the number of cuprate layers in the packets is radically altered. In fact, in this case, in the course of doping, as the broad 2D band is

$\lambda_{pl}(n) \sim \beta(n)$, and have nothing in common with experiment.^{16–18}

5. Of particular interest is the recently synthesized layered compound⁵⁴ $(\text{Ca}_{1-x}\text{Sr}_x)_{1-y}\text{CuO}_2$ with alternating layers of CuO_2 and $\text{Ca}(\text{Sr})$. This compound has a rather high $T_c \approx 110 \text{ K}$. Within the framework of the considered model of close-packed packets (Fig. 2) this corresponds to going to the limit as $n \rightarrow \infty$ and to infinite constants $\lambda_{pl}(n)$ and $\mu_c(n)$, since $\beta(n) \rightarrow \infty$. However, owing to the mutual cancellation of the strong-coupling and local-field effects, the effective coupling constants (59) tends as $n \rightarrow \infty$ to a finite asymptotic value

filled and the l -carrier density \bar{n}_l is increased, the values of k_{F1} and E_{F1} increase but the density parameter $\alpha_l \sim k_{F1}^{-1}$ increases, and with it the coupling constant $\lambda_{pl} \approx \alpha_l$, which turns out to be more substantial than the decrease of the Coulomb pseudopotential μ_c^* owing to the increase of the logarithm $\ln(\tilde{E}_{F1}/\tilde{\omega}_0)$.

Figure 9 shows the dependence of T_c on the dimensionless parameter $\tilde{\kappa}_l = (2\pi \bar{n}_l a^2 d_0)^{1/2}$ for various n at $\tilde{\kappa}_h = 0$ and at the same value of the remaining parameters as in Fig. 4. Evidently the $T_c(\tilde{\kappa}_l)$ dependences do not correspond to the experimental data of Ref. 14 for multilayer cuprate MOC (such as $\text{Bi}_2\text{Sr}_2\text{Ca}_{n-1}\text{Cu}_n\text{O}_x$ or $\text{Tl}_m\text{Ba}_2\text{Ca}_{n-1}\text{Cu}_n\text{O}_x$), and the maximum values of T_c do

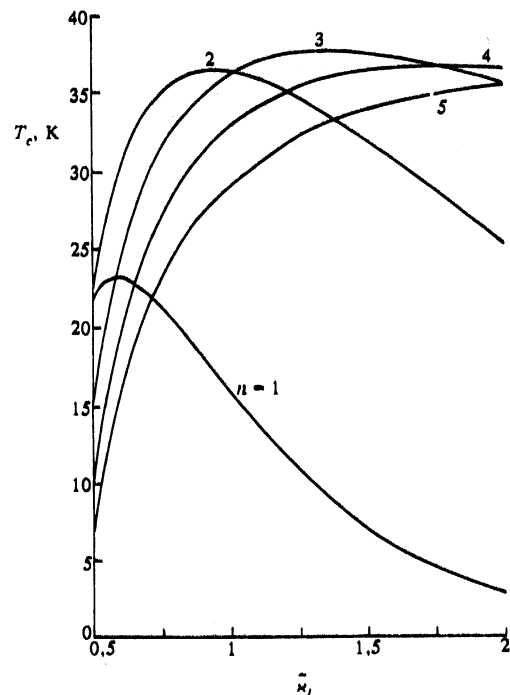


FIG. 9. Dependences of T_c on $\tilde{\kappa}_l$ for various n at $\tilde{\kappa}_h = 0$, i.e., for polar EPhI in the absence of EPI (at the same values of the remaining parameters as in Fig. 4).

not exceed 40 K. Thus, the contribution of the electron-plasmon interactions turns out in the present model to be decisive for HTSC. At the same time, the rapid (exponential) decrease of T_c with increase of $\tilde{\kappa}_l \sim \tilde{n}_l^{1/2}$ at $n = 1$ in Fig. 9 correlates with the abrupt decrease of T_c in $\text{La}_{2-x}(\text{Ba,Sr})_x\text{CuO}_4$ when the dopant content is increased in the region $x > 0.15$, which may indicate a predominant mole of electron-phonon interactions in this cuprate MOC.

7. We proceed to analyze the oxygen IE in the SC phases of cuprate MOC, which tend to suppress the IE with rise of T_c ,^{7,9} in contrast to ordinary superconductors in which the opposite tendency is observed as a rule, with the IE weakening as T_c is lowered until the IE exponent vanishes or reverses sign at $T_c < 1$ K because of the strong Coulomb repulsion at a weak electron-phonon interaction.^{53,86}

An exception among cuprate MOC is $\text{La}_{2-x}\text{Sr}_x\text{CuO}_4$ with an anomalous behavior of the IE exponent for oxygen as a function of the composition, (viz., α_O first increase with increase of the Sr content up to a maximum $\alpha_O \approx 0.6$, and at the point $x = 0.15$ near the maximum of T_c it decreases jumpwise to $\alpha_O \approx 0.1$ (Ref. 87), apparently because of the lattice instability and the anharmonicity of the phonons in the region of the structural transition when the electron-phonon interaction is strong.

The isotopic effect was measured in Ref. 10 with ^{16}O replaced by ^{18}O in the compound $\text{Y}_{1-x}\text{Pr}_x\text{Ba}_2\text{Cu}_3\text{O}_{7-\delta}$, as a function of the content of the Pr dopant that suppresses the superconductivity (lowers T_c). This can be due both to the large magnetic moment of the Pr atoms and to the lowering of the hole density on account of the higher valency of Pr compared with Y, and in this sense a decrease of Pr is equivalent to a decrease of the oxygen deficit δ . It was observed in Ref. 10 that as x is decreased and T_c is increased, with δ constant ($\delta \leq 1$), the IE index decreases from $\alpha_O \approx 0.5$ at $x = 0.5$ and $T_c \approx 30$ K to $\alpha_O \approx 0.02$ at $x = 0$ and $T_c \approx 90$ K (see Fig. 10a).

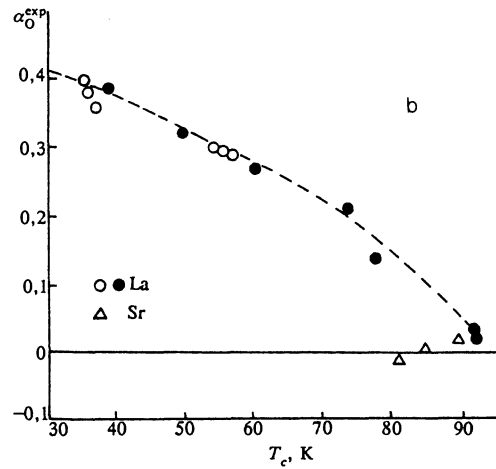
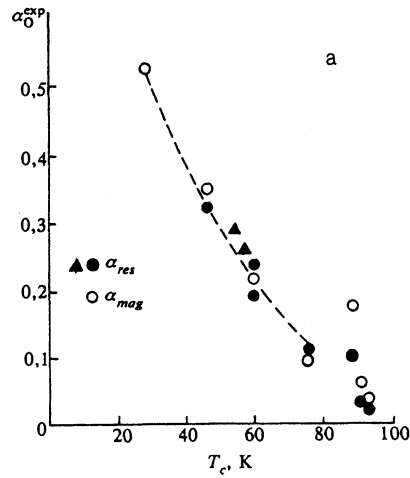


FIG. 10. Experimental plots of the oxygen IE exponent α_O on T_c for the mixed compounds $\text{Y}_{1-x}\text{Pr}_x\text{Ba}_2\text{Cu}_3\text{O}_{7-\delta}$ (a, Ref. 10) and $\text{YBa}_{2-x}(\text{La,Sr})_x\text{Cu}_3\text{O}_{7-\delta}$ (b, Ref. 88).

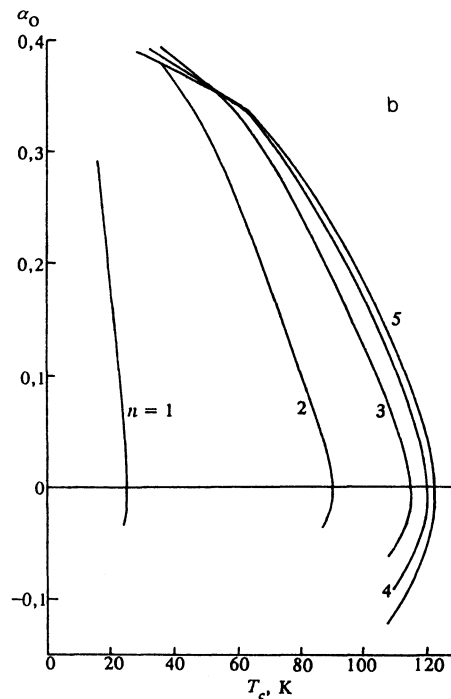
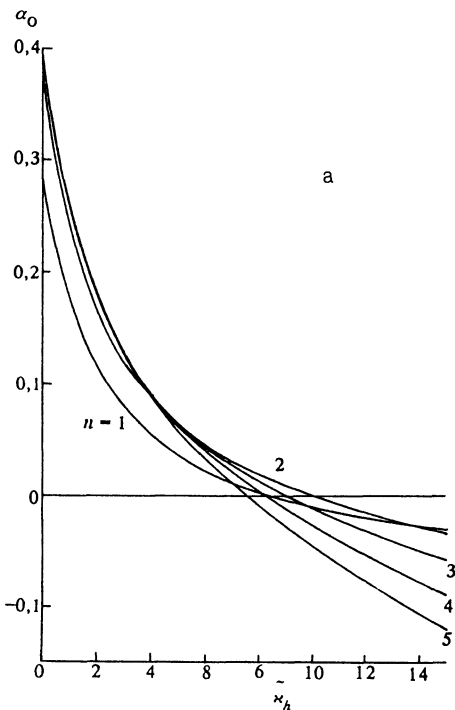


FIG. 11. Dependences of $\tilde{\alpha}_O$ on $\tilde{\kappa}_h$ (a) and on T_c (b) for the parameters of Fig. 4.

A similar result was obtained in Ref. 88 with the Ba in $\text{YBa}_2\text{Cu}_3\text{O}_z$ partially replaced by La, the atoms of which have a higher valency (than Ba) and have no magnetic moment. The oxygen isotopic-effect exponent in $\text{YBa}_{2-x}\text{La}_x\text{Cu}_3\text{O}_z$ compound (with $z \approx 7$) decreased from $\alpha_O \approx 0.4$ at $x = 0.5$ and $T_c \approx 40$ K to $\alpha_O < 0.02$ at $x = 0$ and $T_c \approx 92$ K, and a zero or even negative isotopic effect was observed when Ba was replaced by Sr (see Fig. 10b).

Calculations of the isotopic-effect index in the above "plasmon" mechanism of superconductivity in a layered metal with a narrow 2D band near the Fermi surface, using Eq. (57) and taking Eqs. (48), (51), (52), (56), and (58) into account, show that Coulomb repulsion, owing to the anomaly large (compared with ordinary metals) values of the pseudopotential $\tilde{\mu}_c^* \approx 0.3-0.8$ (see Fig. 5b), leads to strong suppression of the isotopic effect and causes α_O to vanish and reverse sign in the region of maximum T_c , where $\tilde{\mu}_c^* \gtrsim \Lambda$.

Figure 11 shows the dependences of α_O on \tilde{x}_h (a) and on T_c (b), plotted for the parameters of Fig. 4 at various n . As seen from the figure, the oxygen isotopic effect index vanishes and then becomes negative in the region where T_c is lower. It must be emphasized that this is precisely the isotopic-effect anomaly observed in Ref. 88 for $\text{Y}(\text{Ba}_{1-x}\text{Sr}_x)_2\text{Cu}_3\text{O}_z$ (Fig. 10b). The reason may be that the smaller radius of the Sr^{2+} ions (compared with Ba^{2+}) makes possible supersaturation of the samples with oxygen ($z > 7$) and a shift towards higher hole densities, where T_c decreases and $\alpha_O < 0$. A similar reversal of the sign of α_O on passing through the maximum of T_c should be observed in the compounds BiSrCaCuO and TlBaCaCuO .

It is thus possible to explain, on the basis of the "plasmon" mechanism of HTSC, the anomalies of the isotopic effect in cuprate MOC, in agreement with the experimental data.^{10,88}

On the other hand, if the EPI interaction is excluded ($\tilde{\Omega}_h = 0, \tilde{x}_h = 0$) and only the polar EPhI with oxygen vi-

brational modes ω_{LO} and Ω_O , the behavior of the IE changes radically: increases rapidly as \tilde{x}_l increases (Fig. 12a) and as T_c increases (Fig. 12b) from negative values of $\alpha_O \approx -(0.05-0.75)$ at low carrier densities ($\tilde{x}_l = 0.5$) and $T_c \approx 5-20$ K to positive values $\alpha_O \approx 0.25-0.45$ at higher densities ($\tilde{x}_l = 2$) and $T_c \approx 25-40$ K. These dependences agree qualitatively with the character of the IE for ordinary EPhI in low-temperature superconductors,^{9,53,86} but does not agree with experiment for the oxygen IE in cuprate MOC.^{7-10,88}

6. CONCLUSIONS

The following conclusion can be drawn from the foregoing. The proposed model^{21,22} of a layered metal, with quasi-two-dimensional electron spectrum and with two 2D bands having substantially different widths ($W_l \gg W_h$) and overlapping near the Fermi level, can account, on the basis of the standard superconductivity theory with Cooper pairing for the main peculiarities and regularities of HTSC in cuprate MOC in the intermediate coupling approximation ($\Lambda \lesssim 1, T_c \ll \tilde{\omega}_0$). This is due to allowance for factors such as: a) interaction of degenerate l -carriers in a wide band with lf collective excitations of the charge density of almost localized h -carriers in a narrow band (acoustic plasmons) with a spectrum periodic in momentum, b) hybridization of the AP with dipole-active (polar) optical oscillations of oxygen ions, c) multilayer "packet" crystal structure of cuprate MOC with close-packed conducting CuO_2 layers, d) multi-particle Coulomb correlations in a charged quasi-two-dimensional Fermi liquid of l -carriers (of the type of "local-field" effects).

In particular, the experimentally observed nonmonotonic dependence of T_c on the dopant density or on the oxygen content¹¹⁻¹⁵ in this model (Figs. 4 and 7) is the result of competition between the increase of the width of the inter-electron attraction region, on the one hand, and the enhance-

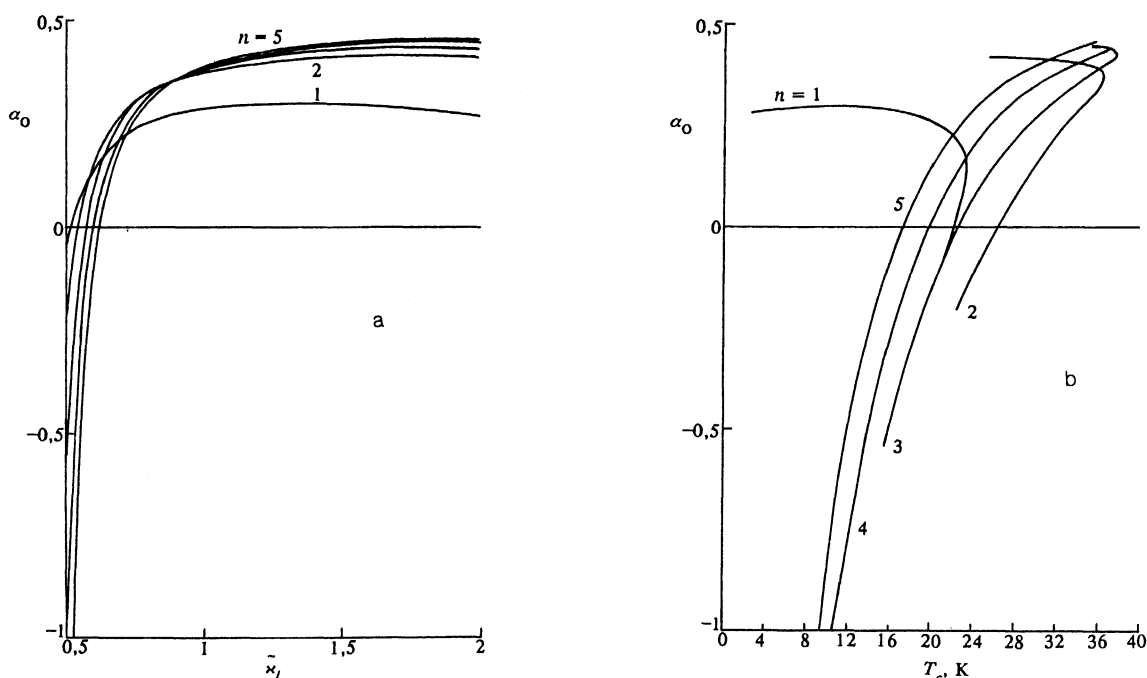


FIG. 12. Dependences of α_O on \tilde{x}_l (a) and on T_c (b) at $\tilde{x}_h = 0$ (in accordance with Fig. 9).

ment of the Coulomb repulsion, on the other, due to the increase of the h -carrier plasma frequency Ω_h and the frequency $\tilde{\Omega}_+$ of the hybrid phonon-plasma oscillations in the course of filling the narrow band with h -carriers at almost constant l -carrier density (due to "pinning" of the Fermi level near the edge of the narrow band with high density of states).

The rise of T_c with increase of the number of cuprate CuO_2 layers in the unit cell of the crystal¹⁶⁻¹⁸ is due to the almost additive contribution of each layer to the EPI constant, owing to the proximity effect, while the tendency to saturation and even to lowering of T_c at sufficiently large n (Fig. 8) is due to the almost full mutual cancellation of the effects of the local field and of the strong coupling.

The abrupt decrease (down to zero and below) of the oxygen isotopic effect with rise of T_c (Fig. 11), which is typical of cuprate MOC^{7-10,88} (Fig. 10) is due to the anomalously strong (compared with ordinary superconductors⁷⁴) Coulomb repulsion on account of the relatively small Bogolyubov-Tolmachev logarithm $\ln(\tilde{E}_{F1}/\tilde{\omega}_0)$ in the Morel-Anderson pseudopotential μ_c^* .

Hybridization of hf oxygen vibrational modes with AP should lead, on the one hand, to an increase of the frequencies of the corresponding peaks of the phonon density of states, which agrees with the results of tunnel and neutron experiments⁴⁶⁻⁴⁸ for HTSC phases of cuprate MOC, and on the other to different anomalies in the phonon dispersion revealed by neutron scattering, and to breaks in the spectra and with frequency jumps in the region of "polariton" splitting of the branches (Fig. 1), inasmuch as neutrons are not scattered by "plasmlike" electron-density perturbations with a quasicoustic dispersion law.¹⁷ However, strong AP damping on account of elastic scattering of h -carriers by charged oxygen vacancies and by non-isovalent impurities (Drude damping) can make the hybridization of AP with

optical phonon unobservable on account of smearing of the phonon peaks. This damping, nonetheless, should not influence the value of T_c so long as the AP lifetime exceeds the l -carrier Cooper-pairing time.

We note in conclusion that the model considered in the present paper makes it possible to predict certain possibilities of further raising T_c , say by increasing the distance d between CuO_2 cuprate layers separated by Ca^{2+} layers and by increasing the number of intermediate dielectric BiO and TlO layers. It seems that this is the very reason why, in multilayer cuprate MOC with BiO or TlO layers in the unit cell, the maximum value $T_c^{\text{max}} \approx 125$ K (at $n = 3$) is higher than in compound with TlO monolayers ($T_c^{\text{max}} \approx 110$ K).

Figure 13a shows plots of T_c vs \tilde{x}_h for the same parameters as in Fig. 4, but with $\delta_0 = 5.25$ ($d = 16.8$ Å), corresponding to introduction into the unit cell of two additional BiO or TlO layers (for example, when single-crystal films are grown by molecular epitaxy). It is seen from the figure that in this case the maximum of T_c at $n = 5$ reaches $T_c^{\text{max}} \approx 155$ K.

Even higher maxima of T_c can be attained by increasing the l -carrier density \bar{n}_l (i.e., the parameter \tilde{x}_l) provided the positions of the Fermi level and of the narrow band coincide (peak of the density of states). Thus, for example, if \bar{n}_l in thallium MOC is increased to $\bar{n}_l = 8 \cdot 10^{21} \text{ cm}^{-3}$ (i.e., $\tilde{x}_l = 1.5$), we obtain $T_c^{\text{max}} \approx 220$ K at $n = 5$ for $\text{Tl}_2\text{Ba}_2\text{Ca}_4\text{Cu}_5\text{O}_x$. This occurs prior to saturation and inversion of T_c with respect to the number n of the cuprate $2D$ CuO_2 layers in the unit cell (cf. Fig. 7).

Thus, according to the considered "plasmon" mechanism of HTSC, simultaneous increase of the parameters \bar{n}_l , d , and n in multilayer cuprate MOC should lead to a substantial rise of T_c of high-temperature superconductors, notwithstanding F. Anderson's^{89,90} known statement that high T_c cannot be obtained with the aid of "electronic" (in par-

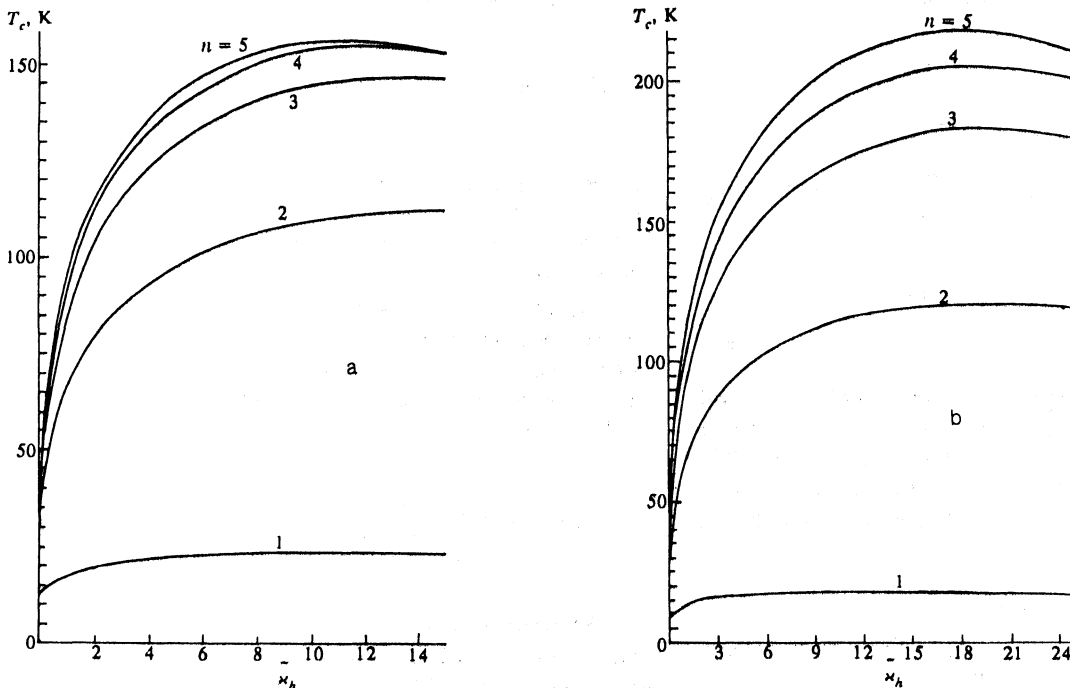


FIG. 13. Dependences of T_c on \tilde{x}_h for hypothetical cuprate MOC with $d = 16.8$ Å (a) when $T_c^{\text{max}} \approx 155$ K at $n = 5$ and with $\tilde{x}_l = 1.5$ (b), when $T_c^{\text{max}} \approx 220$ K at $n = 5$ (the remaining parameters are the same as in Fig. 4).

ticular, an "excitonic," Refs. 91 and 92) superconductivity mechanisms, a statement which is valid only in the random-phase approximation, with allowance for multiparticle Coulomb correlations (of the local-field-effects type) and other factors that enhance the interelectron attraction (ionicity of the lattice, multilayer character of the structure, multivalley character of the band spectrum, and others).

The author thanks A. G. Nazarenko, A. L. Kasatkin, A. É. Pashitskiĭ, and A. V. Semenov for help with the numerical calculations and with the analysis of the literature, and also M. V. Loktev, V. M. Pan, V. B. Timofeev, and G. M. Éliashberg for helpful discussions of various aspects of the HTSC problem, and also E. G. Maksimov for constructive advice.

APPENDIX

In a layered crystal containing several equivalent 2D layers per unit cell,¹⁸⁾ the matrix element of unscreened Coulomb interaction between charges concentrated in the layers can be easily calculated using the summation equation

$$\operatorname{Re} \sum_{m=-\infty}^{\infty} \exp(imz) \exp(-|m|y) = \frac{\operatorname{sh} y}{\operatorname{ch} y - \cos z}. \quad (\text{A1})$$

Thus, for example, let n conducting CuO_2 layers in each unit cell of cuprate MOC of the type $\text{Bi}_2\text{Sr}_2\text{Ca}_{n-1}\text{Cu}_n\text{O}_x$ and $\text{Tl}_m\text{Ba}_2\text{Ca}_{n-1}\text{Cu}_n\text{O}_x$ be gathered into packets, with distance d_0 between the layers in a packet and with distance d between packets of thickness

$$L(n) = (n-1)d_0$$

(Fig. 2), so that the period of the structure (the lattice constant) along the z axis is equal to

$$c(n) = d + L(n).$$

We have then for the Coulomb matrix element in the momentum approximation the expression:

$$V_C(q_{\parallel}, q_z, n) = \frac{2\pi e^2 c(n)}{q_{\parallel}} \left\{ \frac{\operatorname{sh} q_{\parallel} c(n)}{\operatorname{ch} q_{\parallel} c(n) - \cos q_z c(n)} + 2 \sum_{m=1}^{n-1} \cos m q_z d_0 \exp(-m q_{\parallel} d_0) + 2 \sum_{m=1}^{n-1} \cos m q_z d_0 \operatorname{ch}(m q_{\parallel} d_0) \times \left[\frac{\operatorname{sh} q_{\parallel} c(n)}{\operatorname{ch} q_{\parallel} c(n) - \cos q_z c(n)} - 1 \right] \right\}. \quad (\text{A2})$$

For sufficiently large q_{\parallel} , when $q_{\parallel} c(n) \gg 1$ and $m q_{\parallel} d_0 \gg 1$, Eq. (A2) leads with exponential accuracy to expression (6). Note that as $n \rightarrow \infty$ the matrix element (A2) tends to infinity, but the Coulomb potential in real 3D space, which is defined (disregarding Umklapp processes) by the expression

$$V_C(R, z, n) = \int_0^{\infty} \frac{q_{\parallel} dq_{\parallel}}{2\pi} J_0(q_{\parallel} R) \int_{-\pi/c(n)}^{\pi/c(n)} \frac{dq_z}{2\pi} V_C(q_{\parallel}, q_z, n) \exp(iq_z z), \quad (\text{A3})$$

where $J_0(x)$ is a Bessel function, can be readily seen to remain finite as $n \rightarrow \infty$ and $c(n) \rightarrow \infty$ everywhere except at the singular point $R = 0$. The relation $V_C(q_{\parallel}, q_z, n)/c(n)$ is finite as $n \rightarrow \infty$ and goes over, according to (A1), into the known expression for the Coulomb matrix element in a simple layered crystal with layer spacing d_0 (in 2D space):

$$V_C(q_{\parallel}, q_z) = \frac{2\pi e^2}{q_{\parallel}} \frac{\operatorname{sh} q_{\parallel} d_0}{\operatorname{ch} q_{\parallel} d_0 - \cos q_z d_0}. \quad (\text{A4})$$

Finally, at $n = 1$ the ratio $V_C(q_{\parallel}, q_z, 1)/d$ becomes equal to expression (A4) for a crystal with distances d between layers.

We now calculate the structure factors $\beta(n)$ and $\tilde{\beta}(n)$ which are determined by the Fourier component $\Psi_{\perp}(p_z)$ of the transverse part $\Psi_{\perp}(z)$ of the wave function of the carriers in the layers. The presence of the factor $\Psi_{\perp}^2(p_z)$, which is contained in the Green's functions (19) and (21), is due to separation of the variables of the "fast" longitudinal (in the plane of the layers) and "slow" transverse (across the layers) motion of the electrons. This separation is possible in the framework of the "adiabatic" approximation in the case of a sufficiently strong two-dimensional anisotropy of the electron spectrum, when the probability of tunneling between layers is exponentially small, and the cylindrical Fermi surface is weakly rippled along p_z , corresponding to strong anisotropy of the effective masses ($m_{\perp}^*/m_{\parallel}^* \gtrsim 10^2$). Representing in this case the electron (hole) wave function in the 2D layer in the multiplicative form

$$\Psi(\mathbf{r}) = \Psi_{\parallel}(x, y) \Psi_{\perp}(z)$$

and introducing normal and anomalous Green's functions in longitudinal variables at a fixed coordinate z (cf. Ref. 70)

$$G(x - x', y - y'; z) = i \langle \Psi_{\parallel}(x, y) \Psi_{\parallel}^+(x', y') | \Psi_{\perp}(z) |^2 \rangle, \quad (\text{A5})$$

$$F(x - x', y - y'; z) = i \langle \Psi_{\parallel}(x, y) \Psi_{\parallel}(x', y') \rangle \Psi_{\perp}^2(z), \quad (\text{A6})$$

we obtain, after changing to the momentum representation in terms of the independent variables, the expressions (19) and (21) in which the function $\Psi_{\perp}(p_z)$ is assumed for simplicity to be real.

Separating the variables in the normal and anomalous self-energy parts responsible for the EPI and the polar EPhI, and taking (6) or (A2) into account, we can separate the dimensionless structure factor that depends on the number n of the layers:

$$\beta(n) = c(n) \int_{-\pi/c(n)}^{\pi/c(n)} \frac{dp_z}{2\pi} \sum_{K=-\infty}^{\infty} \Psi_{\perp}^2(p_z + \frac{2\pi K}{c(n)}), \quad (\text{A7})$$

The integration over p_z is carried out here within the limits of the first BZ, and the sum over K describes the contribution of the Umklapp processes.

Similarly, to calculate the polarization operator of the l - and h - carriers localized in the 2D layers:

$$\begin{aligned} \Pi(\mathbf{p}, i\omega_n) &= 2T \sum_{\omega_m} \int \frac{d^3 p'}{(2\pi)^3} [G(\mathbf{p}', i\omega_m) G(\mathbf{p}' - \mathbf{p}, i\omega_m - i\omega_n) \\ &+ F(\mathbf{p}', i\omega_m) F(\mathbf{p}' - \mathbf{p}, i\omega_m - i\omega_n)] \\ &\times \Gamma_C(\mathbf{p}' - \mathbf{p}, i\omega_m - i\omega_n; \mathbf{p}, i\omega_n), \end{aligned} \quad (\text{A8})$$

we can also separate a corresponding structure factor [see (7)]

$$\tilde{\beta}(n) = c(n) \int_{-\pi/c(n)}^{\pi/c(n)} \frac{dp_z}{2\pi} \sum_{K=-\infty}^{\infty} \Psi_{\perp}^4(p_z + \frac{2\pi K}{c(n)}, n). \quad (\text{A9})$$

In layered crystals with packet structure of the type of the cuprate MOC $\text{Bi}_2\text{Sr}_2\text{Ca}_{n-1}\text{Cu}_n\text{O}_x$ and $\text{Tl}_m\text{Ba}_2\text{Ca}_{n-1}\text{Cu}_n\text{O}_x$ ($m=1,2$), in which n CuO_2 layers, gathered into dense packets with distance $d_0 = 3.2 \text{ \AA}$ between CuO_2 layers in the packet and with much larger distance $d = 9.6 \text{ \AA}$ between packets in thallium MOC with monolayer TlO ($m=1$) and $d = 12 \text{ \AA}$ in bismuth or thallium MOC with bilayer NiO or TlO ($m=2$), the transverse distribution of the electron (hole) density along the z axis can be specified in the form

$$|\Psi_{\perp}(z)|^2 = A \sum_{i=1}^n \sum_{j=-\infty}^{\infty} \exp\{-|z - z_{ij}|/l_0\}, \quad (\text{A10})$$

where z_{ij} is the coordinate of the i th layer in the j th packet, l_0 is the characteristic length of the exponential decrease of the carrier density with increase of distance from the layer plane, and A is a normalization constant.

We assume hereafter that $d_0 \gg l_0$ but is comparable with the coherence length

$$\xi_{\perp} = \xi_{\parallel} \sqrt{m_{\parallel}^*/m_{\perp}^*},$$

where ξ_{\parallel} is the longitudinal coherence length in the plane of the layers ($\xi_{\parallel} \gg \xi_{\perp}$),⁸⁵ so that a proximity effect arises between the packet layers in the superconducting state. At the same time, since $d \gg d_0 \gtrsim \xi_{\perp}$, a weak (Josephson) coupling exists between the packets. This coupling can be neglected in first-order approximation, and an individual packet can be regarded as a single "thick" superconducting layer of thickness

$$L(n) = (n-1)d_0,$$

with all CuO_2 layers in a coherent superconducting state. This means that in this approximation no account is taken of the periodicity of the layered structure along the z axis, so that it is possible to retain in the sum over j of (A10) only one term with $j=0$. Accordingly, one can disregard in (A7) and (A9) the p_z Umklapp processes and retain in the sum over K only one term with $K=0$.

As a result, calculating the Fourier component of the function

$$|\Psi_{\perp}(z)|^2 \sim \sum_{i=1}^n \exp\{-|z - z_{i0}|/l_0\}$$

with allowance for its normalization to unity at the point $z = z_{i0}$, we obtain

$$\Psi_{\perp}^2(p_z, n = 2k-1) = \frac{1}{1 + (p_z l_0)^2} \left[1 + 2 \sum_{m=1}^{k-1} \cos(mp_z d_0) \right], \quad (\text{A11})$$

$$\Psi_{\perp}^2(p_z, n = 2k) = \frac{1}{1 + (p_z l_0)^2} \sum_{m=1}^k \cos \left[\frac{(2m-1)}{2} p_z d_0 \right]. \quad (\text{A12})$$

For a simple layered crystal with $n=1$, substituting (A11) in (A7) and (A9), we get

$$\beta(1) = \frac{d}{\pi l_0} \text{arctg} \left(\frac{\pi l_0}{d} \right), \quad \tilde{\beta}(1) = \frac{1}{2} \left[\beta(1) + \frac{1}{1 + (\pi l_0/d)^2} \right]. \quad (\text{A13})$$

In the general case $n \neq 1$ and $l_0 \neq 0$, the integrals over p_z in (A7) and (A9), with allowance for (A11) and (A12), cannot be calculated in explicit form. In the limiting case $l_0 = 0$, when $\beta(1) = \tilde{\beta}(1) = 1$, one can obtain for $\beta(n)$ and $\tilde{\beta}(n)$ at $n > 1$:

$$\beta(n) = \begin{cases} 1 + \frac{2c(n)}{\pi d_0} \sum_{m=1}^{k-1} \frac{1}{m} \sin \left[\frac{m\pi d_0}{c(n)} \right], & n = 2k-1, \\ \frac{4c(n)}{\pi d_0} \sum_{m=1}^k \frac{1}{(2m-1)} \sin \left[\frac{(2m-1)\pi d_0}{2c(n)} \right], & n = 2k, \end{cases} \quad (\text{A14})$$

$$\tilde{\beta}(n) = n + \frac{2c(n)}{\pi d_0} \sum_{m=1}^{n-1} \frac{n-m}{m} \sin \left[\frac{m\pi d_0}{c(n)} \right]. \quad (\text{A15})$$

It is easily seen that when $n \gg 1$ and $c(n) \gg \pi d_0$ expressions (A14) and (A15) take with good accuracy the form

$$\beta(n) = n, \quad \tilde{\beta}(n) = n + 2 \sum_{m=1}^{n-1} (n-m) \equiv n^2. \quad (\text{A16})$$

Figure 3 shows plots of $\beta(n)$ and $\tilde{\beta}(n)$ for $l_0 = 0$, $d = 12 \text{ \AA}$ and $d_0 = 3.2 \text{ \AA}$ (b), and also the dependences of $\beta(1)$ and $\tilde{\beta}(1)$ on l_0 (a).

¹⁾This model was used in Refs. 21 and 22 to describe the anomalies of the kinetic, thermodynamic, optical, and magnetoresonance properties of the normal metallic state of cuprate MOC.

²⁾This was demonstrated earlier in Ref. 27 for quasi-one-dimensional (chain) metals with narrow one-dimensional (1D) band, and in Ref. 26 for intermetallic compounds of transitions (such as Nb_3Ge) with a narrow three-dimensional (3D) bands of cubic symmetry, and in Ref. 22 for layered metals with narrow 2D bands.

³⁾Earlier papers³⁷ discussed an "electronic" mechanism of superconductivity in transition metals on account of interband static screening of the Coulomb interaction by s - and d -electrons, without allowance for retardation, i.e., for exchange of virtual If plasmons.

⁴⁾Such a possibility was considered⁴⁵ in connection with the problem of raising T_c in semiconductors (semimetals) with substantially different

masses of the conduction electrons and holes (the so-called "excitonium").

⁵Photoelectron-emission spectra exhibit "pinning" of the Fermi level,^{50,51} which may point to filling a narrow band with a high density of states.

⁶According to Ref. 14, the maximum of T_c for most MOC with hole-type conductivity is observed when the number of doped holes is $x_p = 0.1-0.3$ per Cu_2O cuprate layer in a unit cell, which corresponds for a lattice constant $a \approx 3.8 \text{ \AA}$ to 2D-densities $N_p \approx \chi_p/a^2 \approx (0.7-2.1) \cdot 10^{14} \text{ cm}^{-2}$.

⁷In thallium and bismuth MOC the distance between the cuprate CuO_2 layers separated by Ca layers is $d_0 = 3.2 \text{ \AA}$, as against $d \approx 9.6 \text{ \AA}$ for crystals with a TiO monolayer and $d \approx 12 \text{ \AA}$ for crystals with TiO or BiO bilayers.

⁸This corresponds to strong effective-mass anisotropy which is quite large in single-crystal bismuth and thallium MOC ($m_{\parallel}^*/m_{\perp}^* \approx 10^3$).

⁹The corresponding phonon vertex is $\Gamma_{\text{ph}} = 1$ accurate to terms of order $\sqrt{m_{\parallel}^*/M}$, where M is the average ion mass (see Refs. 69 and 70).

¹⁰It is assumed that $\omega_{\text{max}} > \tilde{E}_{\text{FI}}$ but lies lower than the limit of the strong damping due to interband transitions (see Ref. 67), and also that $\omega_{\text{max}} < \Omega_l$, i.e., it is located in the region of relatively weak Landau damping by l -carriers ($\Omega_l \gg 1 \text{ eV}$).

¹¹Static screening by l -carriers in the region $\omega \sim \omega_{\text{max}} > \tilde{E}_{\text{FI}}$ and $q_{\parallel} \approx 2k_{\text{FI}}$ is suppressed by retardation effect, in contrast to the lf region $\omega \lesssim \Omega_{\pm} (2k_{\text{FI}})$, while the dynamic contribution of h -carriers and of the optical phonons is of the order of $(\tilde{\Omega}_{\pm}/\omega_{\text{max}})^2 \ll 1$ [see Eq. (10)].

¹²It is assumed that the ionicity of the cuprate MOC crystals is due mainly to displacements of oxygen ions, i.e., to hf vibrational oxygen modes. In addition, $\tilde{\epsilon}(q,0)$ contains a large positive contribution due to static screening of the Coulomb interaction by the l - and h -carriers, i.e., $\tilde{\epsilon}(q,0) \gg \epsilon_0$.

¹³A zero-gap state with $\tilde{\Delta}_l(0) = 0$ should be manifested in tunnel experiments as well as in the kinetic and thermodynamic properties.

¹⁴Both lf and hf oxygen peaks with $\omega_{l,0} \approx 300-400 \text{ K}$ and $\Omega_0 \approx 600-900 \text{ K}$ are distinctly observed in the tunnel density of states of the low-temperature superconducting phase of bismuth MOC (Ref. 46) as well as in neutron scattering in the dielectric phase of $\text{YBa}_2\text{Cu}_3\text{O}_6$ (Refs. 47 and 48).

¹⁵It is recognized here that $\omega_{l,0} \sim M_{\text{O}}^{-1/2}$ and $\Omega_0 \sim M_{\text{O}}^{-1/2}$ (where M_{O} is the oxygen-atom mass) and $\tilde{\lambda}_0$ and $\tilde{\lambda}_{\infty}$ depend weakly on M_{O} .

¹⁶We have in mind here the exponential decrease of the carrier density with increase of the distance from the plane of the conducting CuO_2 layers (see Fig. 2). The situation may be substantially different in the case of "bridge" oxygen in $\text{YBa}_2\text{Cu}_3\text{O}_7$, which connects the 2D CuO_2 layers with the 1D chains of CuO .

¹⁷The number of "phononlike" modes in the phonon spectrum is preserved here.

¹⁸In the present model we take into account only conducting CuO_2 layers immersed in a dielectric matrix having a certain permittivity. The influence of nonequivalent layers on Coulomb interaction in layered crystal is taken into account in Ref. 93.

¹*Physical Properties of High-Temperature Superconductors*, D. M. Ginsberg, ed. [Russ. transl.], Mir, Moscow (1991).

²M. K. Wu, J. R. Ashburn, C. J. Torng *et al.*, Phys. Rev. Lett. **58**, 906 (1987).

³P. H. Hor, L. Gao, R. L. Meng *et al.*, *ibid.* **58**, 911 (1987).

⁴M. A. Subramanian, S. S. Torardi, J. C. Calabrese *et al.*, Science **239**, 1015 (1988).

⁵H. Maeda, Y. Tanaka, M. Fukutomi, and T. Asano, Jpn. J. Appl. Phys. **27**, L205 (1988).

⁶Z. Z. Sheng and A. M. Hermann, Nature **332**, 138 (1988).

⁷B. Batlogg, R. J. Cava, L. W. Rupp *et al.*, Phys. Rev. Lett. **61**, 1670 (1988).

⁸H. Katayama-Yoshida, T. Hirooka, T. A. Oyamada *et al.*, Physica C **155**, 481 (1988).

⁹P. B. Allen, Nature **335**, 258 (1988).

¹⁰J. P. Franck, J. Jung, M. A.-K. Mohamed *et al.*, Phys. Rev. B **44**, 5318 (1991).

¹¹O. Fujita, X. Aoki, X. Maeno *et al.*, Jpn. J. Appl. Phys. **26**, 1388 (1987).

¹²J. H. Brewer, E. J. Ansaldo, J. F. Carolan *et al.*, Phys. Rev. Lett. **60**, 1073 (1988).

¹³T. Penney, M. W. Shafer, and N. L. Olson, Physica C **162-164**, 63 (1989).

¹⁴J. B. Torrance, A. Bezing, A. I. Nazzari, and S. S. Parkin, *ibid.* **162-164**, 291 (1989).

¹⁵Y. J. Uemura, G. M. Luke, B. J. Sternlieb *et al.*, Phys. Rev. Lett. **62**, 2317 (1989).

¹⁶S. P. Parkin, Y. Y. Lee, E. M. Engler *et al.*, *ibid.* **60**, 253 (1988).

¹⁷M. Ihara, S. Sugise, M. Hirabayashi *et al.*, Nature **334**, 510 (1988).

¹⁸A. Nakamura, Jpn. J. Appl. Phys. **28**, 2468 (1989).

¹⁹A. A. Bush, I. V. Gladyshev, A. A. Golub *et al.*, Pis'ma Zh. Eksp. Teor. Fiz. **50**, 250 (1989) [JETP Lett. **50**, 279 (1989)].

²⁰M. F. Limonov, Yu. F. Markov, A. G. Panfilov, and B. S. Razbirin, SFKhT **4**, 233 (1991).

²¹E. A. Pashitskiĭ, *ibid.* **3**, 2669 (1990).

²²E. A. Pashitskiĭ, Yu. M. Malozovskiĭ, and A. V. Semenov, Zh. Eksp. Teor. Fiz. **100**, 465 (1991) [Sov. Phys. JETP **73**, 255 (1991)]; Ukr. Fiz. Zh. **36**, 889 (1991).

²³D. Pines, Canad. J. Phys. **34**, 1376 (1956).

²⁴D. Pines and I. R. Schrieffer, Phys. Rev. **124**, 1387 (1961).

²⁵O. V. Konstantinov and V. I. Perel', Fiz. Tverd. Tela **9**, 3061 (1967) [*sic*].

²⁶J. Ruvalds, Adv. Phys. **30**, 677 (1981).

²⁷P. F. Williams and A. N. Bloch, Phys. Rev. B **10**, 1097 (1974).

²⁸D. Pines and F. Nozieres, *Theory of Quantum Liquids*, Benjamin, 1966.

²⁹*Problem of High-Temperature Superconductivity*, V. L. Ginzburg and D. A. Kirzhnits, eds. [in Russian], Nauka, 1977.

³⁰I. G. Bednorz and K. A. Müller, Z. Physik B **64**, 189 (1986).

³¹J. W. Garland, Jr., Phys. Rev. **253**, 460 (1967).

³²H. Frohlich, Phys. Lett. A **26**, 59 (1968), J. Phys. C **1**, 544 (1968).

³³B. T. Geilikman, Fiz. Tverd. Tela **12**, 1881 (1970) [Sov. Phys. Solid State **12**, 1497 (1971)]; Usp. Fiz. Nauk **109**, 65 (1973) [Sov. Phys. Uspekhi **16**, 17 (1973)].

³⁴E. A. Pashitskiĭ, Zh. Eksp. Teor. Fiz. **55**, 2386 (1968); **56**, 662 (1969) [Sov. Phys. JETP **28**, 346 (1969), **29**, 362 (1969)]; Ukr. Fiz. Zh. **14**, 1882 (1969).

³⁵E. A. Pashitskiĭ and Yu. A. Romanov, Ukr. Fiz. Zh. **15**, 1594 (1970).

³⁶E. A. Pashitskiĭ and V. M. Chrnousenko, Zh. Eksp. Teor. Fiz. **60**, 1483 (1971) [Sov. Phys. JETP **33**, 802 (1972)].

³⁷B. T. Geilikman, *ibid.* **48**, 1194 (1965) [**21**, 796 (1965)]; Usp. Fiz. Nauk **88**, 327 (1966) [Sov. Phys. Usp. **9**, 142 (1966)].

³⁸E. A. Pashitskiĭ and V. L. Vinetskiĭ, Pis'ma Zh. Eksp. Teor. Fiz. **46**, Supplement, 124 (1987) [JETP Lett. **46**, Suppl. (1987)].

³⁹V. Z. Kresin, Phys. Rev. B **35**, 8716 (1987).

⁴⁰J. Ruvalds, *ibid.*, p. 8869.

⁴¹J. Ashkenazi, C. J. Kuper, and P. Tyk, Jpn. J. Appl. Phys. **26**, 987 (1987); Sol. St. Commun. **63**, 1144 (1987).

⁴²V. Z. Kresin and H. Moravitz, Phys. Rev. B **37**, 7854 (1988). J. Supercond. **1**, 89 (1988).

⁴³E. A. Pashitskiĭ, Ukr. Fiz. Zh. **33**, 747 (1988); **35**, 1411 (1990); Fiz. Tverd. Tela (Leningrad) **31**, 46 (1989) [Sov. Phys. Solid State **31**, 25 (1989)].

⁴⁴E. A. Pashitskiĭ, V. L. Makarov, and S. D. Tereshchenko, Fiz. Tverd. Tela (Leningrad) **16**, 427 (1974) [Sov. Phys. Solid State **16**, 276 (1974)].

⁴⁵A. A. Abrikosov, Zh. Eksp. Teor. Fiz. **94**, No. 1, 235 (1988) [Sov. Phys. JETP **67**, 1867 (1988)]. J. Less Common Met. **62**, 451 (1978).

⁴⁶S. I. Vedenev and V. A. Stepanov, Pis'ma Zh. Eksp. Teor. Fiz. **49**, 510 (1989) [JETP Lett. **49**, 588 (1989)].

⁴⁷B. Renker, F. Gompf, D. Ewert *et al.*, Physica C **153-155**, 253 (1988).

⁴⁸F. Gompf, E. Gering, B. Renker *et al.*, *ibid.*, p. 274.

⁴⁹G. Bergmann and D. Rainer, Z. Phys. **263**, 59 (1973).

⁵⁰H. Matsuyama, H. Katayama-Yoshida, T. Takahashi *et al.*, Physica C **160**, 557 (1989) [**152-154**, 291 (1990)].

⁵¹T. Takahashi, H. Katayama-Yoshida, H. Matsuyama *et al.*, Phys. Rev. B **39**, 6636 (1989).

⁵²N. Bogolyubov, V. V. Tolmachev, and D. V. Shirkov, *New Method in Superconductivity Theory*, Plenum, 1959.

⁵³P. Morel and P. W. Anderson, Phys. Rev. **125**, 1263 (1962).

⁵⁴M. Azuma, Z. Hiroi, M. Takano *et al.*, Nature **356**, 775 (1992).

⁵⁵M. Gurvitch and A. T. Fiory, Phys. Rev. Lett. **59**, 1337 (1987).

⁵⁶A. Kapitulnik, Physica C **153-155**, 520 (1988).

⁵⁷Z. Schlessinger, R. T. Collins, F. Holzberg *et al.*, Phys. Rev. B **41**, 11237 (1990). Phys. Rev. Lett. **55**, 801 (1990).

⁵⁸I. Furo, A. Janossy, L. Mikhaly *et al.*, Phys. Rev. B **36**, 5690 (1987).

⁵⁹A. J. Arko, R. S. List, R. J. Bartlett *et al.*, *ibid.* **40**, 2268 (1989).

⁶⁰D. M. Newns, M. Rasolt, and P. C. Pattnaik, *ibid.* **38**, 6513 (1988).

⁶¹M. Grilli, C. Castellani, and C. Castro, *ibid.* **42**, 6233 (1990).

⁶²P. M. Newns, M. C. Pattnaik, and C. C. Tsuei, *ibid.* **43**, 3075 (1991).

⁶³M. Tachiki and H. Matsumoto, Progr. Theor. Fiz. Suppl. No. 101, 353 (1990).

⁶⁴S. Ishihara, H. Matsumoto, and M. Tachiki, Phys. Rev. B **42**, 10041 (1990).

⁶⁵B. Ya. Shapiro and A. A. Remova, Physica C **160**, 202 (1989); **164**, 105 (1990).

⁶⁶J. Schrieffer, *Theory of Superconductivity*, Benjamin, 1964.

⁶⁷H. Chen, J. Callaway, and N. E. Brenez, Phys. Rev. B **43**, 383 (1991).

⁶⁸O. V. Dologov and E. G. Maksimov, Usp. Fiz. Nauk **138**, 95 (1982) [Sov. Phys. Usp. **25**, 688 (1982)].

⁶⁹A. B. Migdal, Zh. Eksp. Teor. Fiz. **34**, 1438 (1958) [Sov. Phys. JETP **7**, 996 (1959)].

- ⁷⁰A. A. Abrikosov, L. P. Gor'kov, and I. E. Dzyaloshinskii, *Quantum Field-Theoretical Methods in Statistical Physics*, Pergamon (1965).
- ⁷¹G. M. Eliashberg, *Zh. Eksp. Teor. Fiz.* **38**, 966 (1960); **39**, 1437 (1960) [*Sov. Phys. JETP* **11**, 696 (1961); **12**, 1000 (1961)].
- ⁷²A. Virosztek and J. Ruvalds, *Phys. Rev. B* **42**, 4064 (1990).
- ⁷³P. W. Anderson, *Phys. Chem. Solids* **11**, 26 (1959).
- ⁷⁴W. L. McMillan, *Phys. Rev.* **167**, 331 (1968).
- ⁷⁵R. C. Dynes, *Sol. State Commun.* **10**, 615 (1973).
- ⁷⁶M. V. Medvedev, E. A. Pashitskii, and Yu. S. Pyatiletov, *Zh. Eksp. Teor. Fiz.* **65**, 1186 (1973) [*Sov. Phys. JETP* **38**, 587 (1973)].
- ⁷⁷M. V. Medvedev and Yu. S. Pyatiletov, *Fiz. Met. Metalloved.* **37**, 244 (1974).
- ⁷⁸V. M. Pan, E. A. Pashitskii, and V. G. Prokhorov, *Ukr. Fiz. Zh.* **19**, 1297 (1974); V. M. Pan and V. G. Prokhorov, *Fiz. Met. Metalloved.* **40**, 920 (1975).
- ⁷⁹A. A. Karakozov, E. G. Maksimov, and S. A. Mashkov, *Zh. Eksp. Teor. Fiz.* **68**, 1937 (1975) [*Sov. Phys. JETP* **41**, 971 (1975)].
- ⁸⁰P. B. Allen and R. C. Dynes, *Phys. Rev. B* **12**, 905 (1975).
- ⁸¹S. V. Vonsovskii, Yu. A. Izyumov, and E. Z. Kurmaev, *Superconductivity of Transition Metals and of Their Alloys and Compounds* [in Russian], Nauka (1977).
- ⁸²J. Orenstein, G. A. Thomas, A. J. Miller *et al.*, *Phys. Rev. B* **42**, 6342 (1990).
- ⁸³I. Bozovic, J. H. Kim, J. S. Harris, Jr., and W. Y. Lee, *ibid.* **43**, 1169 (1991).
- ⁸⁴N. Nuker, H. Romberg, S. Hakai *et al.*, *ibid.* **39**, 12379 (1989).
- ⁸⁵L. N. Bulaevskii, V. L. Ginzburg, and A. A. Sobyenin, *Zh. Eksp. Teor. Fiz.* **94**, 247 (1988) [*Sov. Phys. JETP* **67**, 355 (1988)].
- ⁸⁶Yu. S. Pyatiletov, *Fiz. Met. Metalloved.* **39**, 679 (1975).
- ⁸⁷M. K. Crawford, *Physica B* **162-164**, 755 (1989).
- ⁸⁸H. J. Borneman and D. E. Morris, *Phys. Rev. B* **44**, 5322 (1991).
- ⁸⁹M. L. Cohen, P. W. Anderson, *AIP Conf. Proc.* 1972, ed. by D. H. Douglas, NY, 1972, p. 17.
- ⁹⁰P. W. Anderson, *Theories of fullerenes T_c which will not work*, 1991.
- ⁹¹V. L. Ginzburg, *Zh. Eksp. Teor. Fiz.* **47**, 2318 (1964) [*Sov. Phys. JETP* **20**, 1549 (1964)]; *Usp. Fiz. Nauk* **95**, 91 (1968).
- ⁹²D. Allender, J. Bray, and J. Bardeen, *Phys. Rev. B* **7**, 1020 (1973).
- ⁹³A. Griffin, *ibid.* **B 38**, 8990 (1988); **39**, 11503 (1988).

Translated by J. G. Adashko